Since January 2020 Elsevier has created a COVID-19 resource centre with free information in English and Mandarin on the novel coronavirus COVID-19. The COVID-19 resource centre is hosted on Elsevier Connect, the company's public news and information website.

Elsevier hereby grants permission to make all its COVID-19-related research that is available on the COVID-19 resource centre - including this research content - immediately available in PubMed Central and other publicly funded repositories, such as the WHO COVID database with rights for unrestricted research re-use and analyses in any form or by any means with acknowledgement of the original source. These permissions are granted for free by Elsevier for as long as the COVID-19 resource centre remains active.

Trends in Analytical Chemistry 161 (2023) 117000

Contents lists available at ScienceDirect

Trends in Analytical Chemistry

journal homepage: www.elsevier.com/locate/trac

CRISPR techniques and potential for the detection and discrimination of SARS-CoV-2 variants of concern

Huyan Xiao [1], Jianyu Hu [1], Camille Huang, Wei Feng, Yanming Liu, Teresa Kumblathan, Jeffrey Tao, Jingyang Xu, X. Chris Le*, Hongquan Zhang**

Division of Analytical and Environmental Toxicology, Department of Laboratory Medicine and Pathology, Faculty of Medicine and Dentistry, University of Alberta, Edmonton, Alberta, T6G 2G3, Canada

ARTICLE INFO

Article history:
Received 31 December 2022
Received in revised form
21 February 2023
Accepted 21 February 2023
Available online 2 March 2023

Keywords:
Bioanalytical assays
Cas proteins
COVID-19
CRISPR
crRNA
Molecular diagnostics
Nucleic acids
Point-of-care test
Ribonucleoprotein
SARS-CoV-2 variants

ABSTRACT

The continuing evolution of the SARS-CoV-2 virus has led to the emergence of many variants, including variants of concern (VOCs). CRISPR-Cas systems have been used to develop techniques for the detection of variants. These techniques have focused on the detection of variant-specific mutations in the spike protein gene of SARS-CoV-2. These sequences mostly carry single-nucleotide mutations and are difficult to differentiate using a single CRISPR-based assay. Here we discuss the specificity of the Cas9, Cas12, and Cas13 systems, important considerations of mutation sites, design of guide RNA, and recent progress in CRISPR-based assays for SARS-CoV-2 variants. Strategies for discriminating single-nucleotide mutations include optimizing the position of mismatches, modifying nucleotides in the guide RNA, and using two guide RNAs to recognize the specific mutation sequence and a conservative sequence. Further research is needed to confront challenges in the detection and differentiation of variants and sublineages of SARS-CoV-2 in clinical diagnostic and point-of-care applications.

© 2023 Published by Elsevier B.V.

1. Introduction

CRISPR (clustered regularly interspaced short palindromic repeats) systems have revolutionized genetic manipulation, cell regulation, and molecular imaging [1–5]. The class 2 CRISPR-associated (Cas) enzymes, including Cas9, Cas12, and Cas13, constitute a single effector protein and have been widely used for genome engineering, whereas the class 1 Cas enzymes comprise a complex of multiple effector proteins [6]. Cas proteins are RNA-guided, switchable nucleases. These nucleases rely on a CRISPR RNA (crRNA) to recognize specific nucleic acid targets. A crRNA for Cas12 and Cas13, or sgRNA for Cas9, generally consists of two main functional domains: a conservative domain that binds to the Cas protein and a programmable domain, often termed spacer, that is designed to recognize the nucleic acid target and hybridize to the target sequence. To recognize the nucleic acid target, the Cas protein first binds to its crRNA, forming a crRNA-Cas ribonucleoprotein (RNP) complex [7–10]. The RNP interacts with the nucleic acid target through the hybridization of the spacer in the crRNA to its complementary sequence in the target. The binding of the target to the RNP switches on the nuclease activity of the Cas protein, cleaving the target nucleic acids [7–10]. Simply altering the spacer sequence of the crRNA allows the Cas nucleases to target and cleave various genomic loci. Thus, the CRISPR-Cas system is simpler and more efficient than other genome-editing nucleases, such as meganucleases [11], zinc-finger nucleases (ZFNs) [12], and transcription activator-like effector nucleases (TALENs) [13]. Meganucleases, ZFNs, and TALENs require protein engineering to edit each target genomic sequence.

In addition to their applications in genomic engineering, CRISPR-Cas systems also advance molecular diagnostics [14–18]. By taking advantage of the simple RNA-guided target recognition and switchable nuclease activity of the CRISPR-Cas systems, researchers have developed various CRISPR-based diagnostic methods for the

* Corresponding author.
** Corresponding author.
E-mail addresses: xc.le@ualberta.ca (X.C. Le), hongquan@ualberta.ca (H. Zhang).
[1] These authors contributed equally.

https://doi.org/10.1016/j.trac.2023.117000
0165-9936/© 2023 Published by Elsevier B.V.

detection of nucleic acids [14–18]. Base-pairing of crRNA with nucleic acid targets ensures the specific recognition of targets and switches on the nuclease activity of Cas effectors. The products of Cas nuclease activity are then detected using various methods, including fluorescence [19,20], electrochemistry [21,22], colorimetry [23,24], and their combination with lateral flow assays [25].

Cas9 targets double-stranded DNA (dsDNA) proximal to a specific protospacer adjacent motif (PAM) [1]. Cas12 targets both single-stranded DNA (ssDNA) and dsDNA adjacent to a PAM [26,27], and Cas13 targets ssRNA [28,29]. This diversity allows for the detection of different types of nucleic acids with corresponding Cas nucleases. Unlike Cas9 nucleases that display one endonuclease activity only cleaving the specific bound targets, Cas12 and Cas13 nucleases have an additional *trans*-cleavage activity that cleaves ssDNA or ssRNA sequences indiscriminately with a high turnover number [27,29]. The multiple turnover *trans*-cleavage activity of Cas12 and Cas13 allows signal amplification. Therefore, assays based on Cas12 and Cas13 nucleases generally have better sensitivity than those based on Cas9 nucleases [18]. These direct assays for nucleic acids have typical limits of detection at pM concentrations [30,31]. For the detection of nucleic acid targets at lower concentrations, Cas nucleases have been incorporated into nucleic acid amplification techniques. One common approach used Cas systems to recognize the products (amplicons) of nucleic acid amplification reactions, and the second approach used Cas enzymes to develop new isothermal amplification techniques [27,30,32]. For example, two pioneering CRISPR-based nucleic acid detection methods, SHERLOCK (specific high-sensitivity enzymatic reporter unlocking) [30] and DETECTR (DNA endonuclease-targeted CRISPR *trans* reporter) [27], combine recombinase polymerase amplification (RPA) or loop-mediated isothermal amplification (LAMP) with Cas13 or Cas12 systems, respectively. In these nucleic acid amplification assays, Cas systems often play three roles: improving detection specificity, transducing amplicons into readout signals, and enhancing detection sensitivity [15].

For the simple and rapid testing of COVID-19, Cas nucleases have been used directly or have been incorporated into nucleic acid amplification techniques for the detection of SARS-CoV-2 viral RNA [33–36]. Complementing the standard RT-PCR diagnostics, CRISPR-based methods have been developed with the aim of potential point-of-care applications. Recently, CRISPR-Cas systems have been increasingly used in the development of assays for the differentiation and detection of SARS-CoV-2 variants of concern (VOCs). Many challenges have been encountered, especially in differentiating the specific variants. Differentiation of SARS-CoV-2 variants often requires discrimination of specific single-nucleotide mutations. However, the specificity of native CRISPR-Cas systems is commonly not sufficient to fulfill the diagnostic requirements for detection of specific variants. Ideally, readout signals should come from the specific variant only but not from other variants or the wild-type SARS-CoV-2. This level of discrimination is challenging for most CRISPR-Cas systems. Therefore, different strategies have been proposed to improve the specificity of CRISPR-Cas systems for the effective detection of SARS-CoV-2 variants.

Although CRISPR-based techniques for the detection of the wild-type SARS-CoV-2 RNA and other nucleic acids have been thoroughly reviewed, there is no critical assessment of recent CRISPR-based techniques aimed at detecting variants. Here, we summarize the recent progress in using CRISPR-based technologies for the detection of SARS-CoV-2 variants. We discuss challenges faced by the current CRISPR-based techniques in discriminating single-nucleotide mutations in the spike protein gene of different SARS-CoV-2 variants. We highlight the main strategies to improve the specificity of CRISPR-Cas systems for the differentiation of SARS-CoV-2 variants.

2. SARS-CoV-2 variants of concern (Alpha, Beta, Gamma, Delta, and Omicron)

The SARS-CoV-2 virus, belonging to the beta coronavirus family, contains a proofreading enzyme to maintain the fidelity of its genome replication [37]. Therefore, SARS-CoV-2 has a relatively lower mutation rate compared to other RNA viruses. However, its high infection rate and the large number of infection cases around the world greatly accelerated its evolution. During the past three years, several dominant variants of SARS-CoV-2 have emerged and become widespread. The World Health Organization (WHO) classified at least five variants of concern (VOCs) on the basis of their higher infection rates, increased severity of symptoms, and/or potential of immune escape [38]. These five VOCs, Alpha, Beta, Gamma, Delta, and Omicron, correspond to the lineages B.1.1.7, B.1.351, P.1, B.1.617.2, and B.1.1.529, respectively, according to the Pango nomenclature system [39]. The Alpha, Delta, and Omicron variants became dominant sequentially throughout the world, while the Beta and Gamma variants spread out regionally [40]. These variants often contain multiple mutation sites in the gene sequence of the spike (S) protein, which lead to changes in infectivity, severity of symptoms, response to vaccination, and immune escape. The discrimination of variants relies mainly on the identification of variant-specific mutations in the S protein gene.

2.1. Structure and function of the spike protein

The S protein (1273 amino acids, aa), a transmembrane protein located on the surface of the virion, mediates the entry of the SARS-CoV-2 virus into the host cells (Fig. 1A and B) [41–43]. The S protein contains two subunits, a receptor binding subunit S1, and a membrane fusion subunit S2, which are separated by the S1/S2 cleavage site (aa 685/686) (Fig. 1D) [44]. The S1 subunit (aa 13–685) consists of two subdomains, an N-terminal domain (NTD) (aa 13–304) involved in the structural conformation of the S protein and a receptor binding motif (RBM, aa 438–508) containing a C-terminal receptor binding domain (RBD, aa 319–541) that is involved in the recognition and binding of the angiotensin-converting enzyme 2 (ACE2) receptor on the cell surface [44]. The S2 subunit (aa 686–1273) consists of five subdomains, a fusion peptide (FP, aa 788–806) that interacts with the cell membrane as RBD binds to the ACE2 receptor, two heptad repeat subdomains (HR1 aa 918–983, HR2 aa 1162–1203) that allow the virion to enter the cell as a whole particle, a transmembrane domain that anchors the S protein on the SARS-CoV-2 virion, and a C-terminal domain that is located inside the virion [44,45].

The entry of a SARS-CoV-2 virion into a host cell starts with the binding of the RBD of the S protein to the ACE2 receptor on the cell surface [43]. Afterward, the transmembrane protease serine 2 (TMPRSS 2) primes the spike protein by cleaving it at the S1/S2 site, exposing the FP region to fuse the viral and host cell membranes [41,43]. Because the S protein has high antigenicity and is vital for viral infection, it has been used as a target for vaccines [46] and therapeutic drugs [47,48]. The S protein and its gene have also been used as targets for the detection of SARS-CoV-2.

Mutations in the S protein can affect not only the infectivity of the virus but also the efficacy of neutralizing antibodies (NAbs) and vaccines. For example, mutations in the RBD domain of the S protein may increase its binding affinity to ACE2, facilitating the cell entry of the virion and enhancing the transmissibility of the virus [49]. On the other hand, the binding affinity of the S protein to NAbs may be reduced due to mutations in the S protein, resulting in decreased efficacy of NAb-based therapies and vaccines [50].

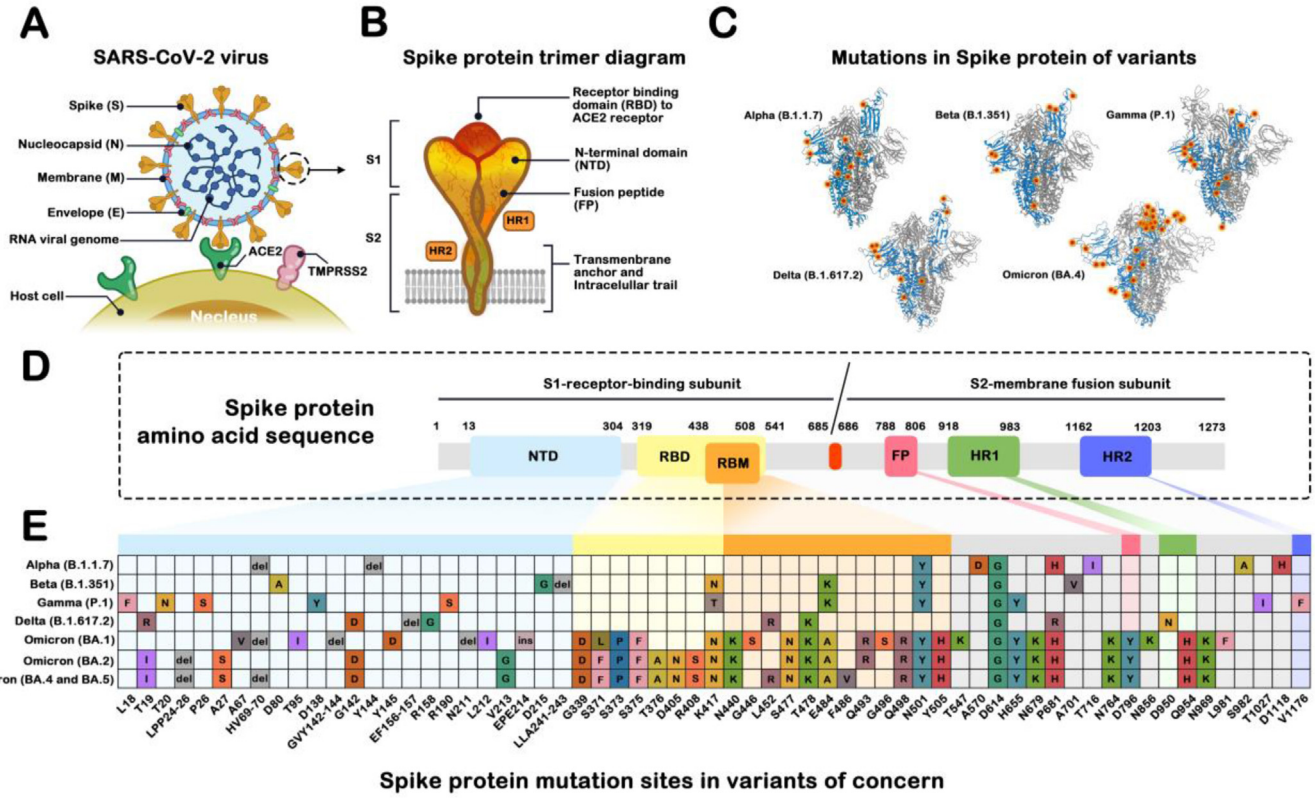

Fig. 1. Structure and composition of the spike (S) protein and related mutation sites in variants of concern. **A.** The typical structure of a SARS-CoV-2 virion and the entry of the virion into the host cell through the interaction between the S protein and cell surface receptor ACE2. **B.** A diagram of the *trans*-membrane S protein homotrimer in which each S protein contains two subunits (S1 and S2) with different functional domains. **C.** The distribution of the mutation sites on a single S protein in different variants. The orange dots denote the locations of mutation in one spike monomer. The 3D structures of the SARS-CoV-2 S protein were obtained from the Protein Data Bank [51]. The IDs of these structures are 7LWV (Alpha), 7LYN (Beta), 8DLO (Gamma), 7W92 (Delta), and 7XNQ (Omicron BA.4). The sites of mutation were noted according to the locations of mutations on S protein demonstrated on the CoVariants [52]. **D.** The locations of the key functional domains in the amino acid sequence of the S protein. **E.** The defining amino acid mutations of different variants within the S protein and the corresponding locations. Data are from the CoVariants [52].

2.2. Five variants of concern and their featured mutations in the S protein

The Alpha variant (B.1.1.7), first identified in the United Kingdom in the fall of 2020 [38], is characterized by multiple amino acid changes compared with the original strain; 10 mutations are located in the S protein (Fig. 1C and E) [52]. For example, the N501Y mutation is in the RBD of the S protein, in which the asparagine (N) at position 501 is replaced by tyrosine (Y). It has been demonstrated that this mutation improved the binding affinity of the RBD to the ACE2 receptor and therefore increased the transmissibility of the virus [53,54]. This mutation is also shared by other VOCs except for the Delta variant. The D614G mutation leads to an increase in the infectivity of the virus [55,56], and is shared by all five VOCs. The Alpha variant also contains three important NTD deletions: the Y144 deletion that may affect the binding of NAbs to NTD [57,58] and the HV69-70 deletions that can increase cell infection [59,60]. Due to these multiple mutations, the Alpha variant shows a 50−100% increase in the reproduction number [61], much higher viral loads in upper-respiratory specimens [62], and around 61% increase in the death rate compared to the pre-existing variants [63].

The Beta variant (lineage B.1.351), first reported in South Africa in May 2020 [38], contains 10 mutations in the spike protein with 3 key substitutions located in the RBD domain (K417N, E484K, and N501Y) and five in the NTD [52,64] (Fig. 1C and E). The three mutations in the RBD domain increase the affinity of the RBD of the Beta variant to the ACE2 receptor by about 20−fold compared to the original strain [65]. The E484K mutation was also reported to impact the NAb binding and reduce the efficacy of RBD targeting NAb [65,66]. The mutations in NTD also reduce the efficacy of NAb binding to NTD [58]. Overall, the Beta variant not only has a transmission rate increased by 50% compared to other variants circulating in the same region by that time [67] but it also shows resistance to the sera antibodies induced by previous infection and vaccination [58,68].

The Gamma variant (P.1), first reported in Brazil in November 2020 [38], contains 12 mutations in the spike protein [52] (Fig. 1C and E). Three mutations in the RBD, K417T, E484K, and N501Y, increase the binding affinity of the Gamma variant to the ACE2 receptor in the same way as the Beta variant [69]. The L18F substitution in the NTD affects the binding of NAbs with the NTD [57]. The Gamma variant is estimated to have a 1.7−2.4 fold increase in transmissibility [69], causes higher mortality even in young adults (aged between 20 and 39 years) [70], and is more resistant to antibodies induced by either previous infection or vaccination, compared to the Alpha variant [68].

The Delta variant (B.1.617.2), which emerged in India in October 2020 [38], has 10 mutations in the S protein (Fig. 1C and E) [52], including two RBD mutations, L452R and T478K, and a furin protease cleavage site proximal mutation P681R. Although the Delta variant does not contain the N501Y mutation that enhances the binding of RBD to the ACE2 receptor, the L452R and T478K mutations have been demonstrated to increase the binding affinity of the

RBD to the ACE2 [71]. The L452R mutation is thought to be related to the decreased sensitivity to NAbs [72]. The P681R mutation facilitates the membrane fusion and internalization of the virus, leading to stronger transmissibility [71,73]. People infected with the Delta variant were reported to have 1000 times higher viral load when first tested as PCR-positive than those affected by the original strain [74]. Overall, the Delta variant shows stronger transmissibility than the Alpha variant [73,75]. Additionally, the Delta variant reduces the efficiency of antibodies and causes a higher vaccine breakthrough infection than other variants [73,76]. A higher hospitalization rate and death rate were observed with the Delta variant than with the Alpha variant [77].

The Omicron variant (B.1.1.529) has several distinct sublineages, including BA.1, BA.2, BA.4, BA.5, XBB.1.5, and XBB.1.x, emerging in multiple countries since November 2021 [38]. BA.1, first reported in southern Africa in November 2021, contains over 30 mutations in the S protein, with 15 mutations located at the RBD (as shown in Fig. 1C and **E)** [52,78]. BA.2, reported at almost the same time as BA.1, shares 20 mutations in the S protein with BA.1 but with several different RBD mutations and distinct NTD mutations [79–81]. BA.2 shows a little higher transmissibility and slightly lower or similar severity of the disease than BA.1 [82]. BA.4 and BA.5, identified in December 2021, share an identical sequence in the S protein and are closely related to BA.2 with a difference of five amino acids, but are more pathogenic than BA.2 [82,83]. All four lineages contain the same key S mutations, T478K, E484A, Q498R, N501Y, Y505H, D614G, H655Y, N679K, and P681H. The RBD mutations T478K and Q498R enhance the binding of the S protein with the ACE2 receptor [84]. These two mutations, together with E484A and Y505H, decrease the binding affinity of NAbs to RBD [84]. Three furin cleavage site proximal mutations, H655Y, N679K, and P681H, may increase the cleavage of the spike protein trimer and favor the entry of the virus into cells, thus enhancing the transmissibility [85]. The Omicron variant shows stronger transmissibility and a higher rate of reinfection than the Beta and Delta variants [86] and can escape the NAb response [78,85,87,88]. On the other hand, disease severity and hospitalization rate caused by the Omicron variant are lower than those caused by the Delta variant [89]. The lower hospitalization rates and disease severity with the Omicron variant may be partially attributable to the prior exposure of the population through infections and/or multiple immunizations, in addition to the virus-specific characteristics. The Omicron variant became the dominant variant soon after it emerged [85]. BA.4 and BA.5 have stronger transmissibility than BA.2 and an increased immune escape for both three vaccine doses and infections from BA.1 and BA.2 [90,91], while the disease severity is similar to that caused by BA.1 [92].

2.3. Mutations used for differentiation and detection of specific variants

Genomic sequences of SARS-CoV-2 and its variants are usually obtained through whole genome sequencing. On the basis of the genomic sequences, different techniques have been developed for the detection of variants. The main features of three groups of techniques, sequencing [93–97], mutation-specific RT-PCR [98–100], and CRISPR-based methods, are summarized and compared (Table S1). In general, sequencing-based methods can provide high-resolution information of the whole genome or a particular gene, enabling the identification of new variants. On the other hand, sequencing methods are usually expensive, time- and labor-intensive, and require personnel with bioinformatics expertise for data analysis. RT-PCR methods have high sensitivity and specificity, and are routinely used in clinical laboratories. RT-PCR methods can be designed for the detection and discrimination of single-nucleotide mutations, and therefore, are suitable for the detection of specific variants. CRISPR-based methods can be performed isothermally, and do not require sophisticated equipment. Thus, CRISPR-based methods have promising potential for point-of-care testing. Fig. 2 lists mutations in the S gene (code for the spike protein) that have been targeted in the development of CRISPR-based assays for the differentiation and detection of VOCs of SARS-CoV-2. The complete S gene mutations in the genome sequences of five VOCs are summarized in Table S2.

Differentiation and detection of variants are often achieved through the detection of mutations that are specific to the particular variant. The selection of specific mutations as targets for the detection of variants is critical. Because the mutation D614G was shared by all five VOCs and N501Y was also shared by four VOCs (except the Delta variant), these two mutations were often targeted in CRISPR-based assays [101–106]. However, the detection of targets containing these two mutations can only differentiate VOCs from the original (wild-type) strain but cannot differentiate among the five VOCs. To discriminate VOCs from each other, researchers often select a specific mutation unique to each variant. For example, the Alpha-specific mutation S982A and Delta-specific mutation D950N were used for the discrimination of these two variants [107]. For the discrimination of multiple variants, multiple mutation sites need to be selected carefully as many variants share the same mutations. Arizti-Sanz et al. [108] reported the discrimination of the five VOCs using multiple mutation sites: HV69–70del for Alpha, K417N for Beta, K417T for Gamma, either L452R or EF156–157del plus R158G for Delta, and GVY142–144del plus Y145D for Omicron. The specific mutations used for the discrimination of each variant in reported CRISPR-based assays are listed in Table S3.

Three main types of Cas proteins, Cas9, Cas12 and Cas13, have been used to develop CRISPR-based methods for the differentiation and detection of SARS-CoV-2 variants. These Cas proteins differ in their nuclease performance. For example, they have different requirements for a PAM sequence; they have different preferences for nucleic acid targets and substrates; and they have different cleavage activities and specificities (Table S4). Correspondingly, these Cas proteins have been incorporated into different approaches for the detection of SARS-CoV-2 RNA, and different strategies have been used to improve the specificity of these Cas proteins for the differentiation of variants. We therefore organized these CRISPR-based methods into three groups based on the type of Cas protein used in the method. In the following sections, we discuss separately the corresponding strategies to improve the specificity of each Cas system for the detection of variants.

3. CRISPR-Cas9-based methods for the detection of variants

CRISPR-Cas9 systems are the first type of Cas nucleases discovered and used for genome editing [1,2]. Earlier CRISPR-based diagnostic methods used mainly Cas9 nucleases to achieve the detection of nucleic acids [14,109]. A typical CRISPR-Cas9 system consists of two components: a Cas9 protein and a single-guide RNA (sgRNA) formed by fusing a crRNA with a *trans*-activating CRISPR RNA (tracrRNA) [1]. The sgRNA contains a conservative stem-loop region for binding to the Cas9 protein and a spacer sequence for hybridizing with the DNA targets. To achieve the nuclease activity, the Cas9 protein first binds to the stem-loop region of the sgRNA and forms a sgRNA-Cas9 RNP [8,110]. This RNP screens dsDNA sequences and finds an adjacent PAM motif, typically a 5′-NGG-3′ sequence. Following the PAM recognition, the spacer sequence within the sgRNA hybridizes to the PAM proximal seed region of the complementary strand on the target DNA, while the Cas9 protein helps to stabilize the non-target DNA strand through the formation

	Alpha (B1.1.7)	Beta (B1.351)	Gamma (P.1)	Delta (B.1.617.2)	Omicron (BA.1)	Omicron (BA.2)	Omicron (BA.4 and BA.5)	Mutation site	Gene sequence (5'-3')	
									Original sequence	Mutated sequence
L18			F					L18F	tgt gtt aat CTT aca acc	tgt gtt aat TTT aca acc
P26			S					P26S	caa tta ccc CCT gca tac	caa tta ccc TCT gca tac
A67					V			A67V	tgg ttc cat GCT ata cat	tgg ttc cat GTT ata cat
HV69-V70	del				del		del	HV69-70del	cat gct ATA CAT GTC tct ggg	cat gct A__ ___ _TC tct ggg
D80		A						D80A	act aag agg ttt GAT aac cct	act aag agg ttt GCT aac cct
G142				D		D	D	G142D	ttt ttg GGT gtt tat tac cac	ttt ttg GAT gtt tat tac cac
Y144	del							Y144del	ttg ggt gtt TAT tac cac	ttg ggt gtt ___ tac cac
Y145					D			Y145D	ggt gtt tat TAC cac aaa	ggt gtt tat GAC cac aaa
EF156-157 R158				del G				EF156-157del +R158G	atg gaa agt GAG TTC AGA gtt tat	atg gaa agt G__ ___ _GA gtt tat
S371					L	F	F	S371L	cta tat aat TCC gca tca ttt tcc	cta tat aat CTC gca tca ttt tcc
								S371F	cta tat aat TCC gca tca ttt tcc	cta tat aat TTC gca tca ttt tcc
S373					P	P	P	S373P	tcc gca TCA ttt tcc act	tcc gca CCA ttt tcc
S375					F	F	F	S375F	gca tca ttt TCC act ttt	gca tca ttt TTC act ttt
K417		N	T		N	N	N	K417N	caa act gga AAG att gct	caa act gga AAT att gct
								K417T	caa act gga AAG att gct	caa act gga ACG att gct
L452				R			R	L452R	aat tac CTG tat aga ttg ttt	aat tac CGG tat aga ttg ttt
S477					N	N	N	S477N	cag gcc ggt AGC aca cct	cag gcc ggt AAC aca cct
T478				K	K	K	K	T478K	gcc ggt agc ACA cct tgt	gcc ggt agc AAA cct tgt
E484		K	K		A	A	A	E484A	aat ggt gtt GAA ggt ttt	aat ggt gtt GCA ggt ttt
								E484K	aat ggt gtt GAA ggt ttt	aat ggt gtt AAA ggt ttt
Q493					R	R		Q493R	cct tta CAA tca tat ggt	cct tta CGA tca tat ggt
G496					S			G496S	caa tca tat GGT ttc caa	caa tca tat AGT ttc caa
Q498					R	R	R	Q498R	tat ggt ttc CAA ccc act	tat ggt ttc CGA ccc act
N501	Y	Y	Y		Y	Y	Y	N501Y	ccc act AAT ggt gtt ggt tac	ccc act TAT ggt gtt ggt tac
D614	G	G	G	G	G	G	G	D614G	ctt tat cag GAT gtt aac	ctt tat cag GGT gtt aac
H655			Y		Y	Y	Y	H655Y	ggg gct gaa CAT gtc aac	ggg gct gaa TAT gtc aac
P681	H			R	H	H	H	P681H	aat tct CCT cgg cgg gca cgt	aat tct CAT cgg cgg gca cgt
								P681R	aat tct CCT cgg cgg gca cgt	aat tct CGT cgg cgg gca cgt
T716	I							T716I	gcc ata ccc ACA aat ttt	gcc ata ccc ATA aat ttt
D950				N				D950N	ctt gga aaa ctt caa GAT gtg	ctt gga aaa ctt caa AAT gtg
N969					K	K	K	N969K	caa ctt agc tcc AAT ttt	caa ctt agc tcc AAA ttt
L981					F			L981F	gat atc CTT tca cgt ctt	gat atc TTT tca cgt ctt
S982	A							S982A	atc ctt TCA cgt ctt gac aaa	atc ctt GCA cgt ctt gac aaa

Fig. 2. Typical S protein and S gene mutations that have been targeted in CRISPR-based assays for the discrimination and detection of variants of concern. Nucleotide sequences of the original strain and variants of SARS-CoV-2 were obtained from the NCBI database. Further details are included in Table S1.

of an R-Loop. The target binding event switches on the nuclease activity of the Cas9. The nuclease sites in the HNH and RuvC domains cleave the target and non-target strands respectively, producing a blunt dsDNA break 3–4 nt upstream of the PAM [1,111]. Mutating either the HNH or the RuvC domain of Cas9 results in a nickase (nCas9) that generates a single strand break [112], while mutating both domains results in "dead Cas9" (dCas9) which maintains the RNA-guided DNA binding ability, but does not cleave the target [113].

Although the Cas9 system is sequence-specific, a single nucleotide mismatch between the spacer sequence of the sgRNA and the target sequence may not be sufficient to completely inhibit the Cas9 nuclease activity, depending on the mismatch position. The PAM-proximal mismatches are less tolerable than the PAM distal mismatches for the sgRNA-guided target recognition of the Cas9 system [114,115]. More mismatches between the spacer and target sequences decreased the affinity of RNP binding to the target [116]. Shortening the crRNA by 2–3 nucleotides at the 5′ end (truncated crRNA) increased the specificity [117,118]. Extension by adding two additional G nucleotides to the 5′ end and chemical modifications (e.g., 2′-F ribose modification) of crRNA reduced the off-target effect of CRISPR-Cas9 [119–121]. In addition, engineering a hairpin secondary structure in the spacer of crRNA increased the specificity by several orders of magnitude [122].

For Cas9-based detection of SARS-CoV-2 variants, the viral RNA was first reverse transcribed and amplified to generate DNA amplicons (Fig. 3A), and the amplicons were recognized by Cas9. Two strategies have been used to improve the specificity: targeting

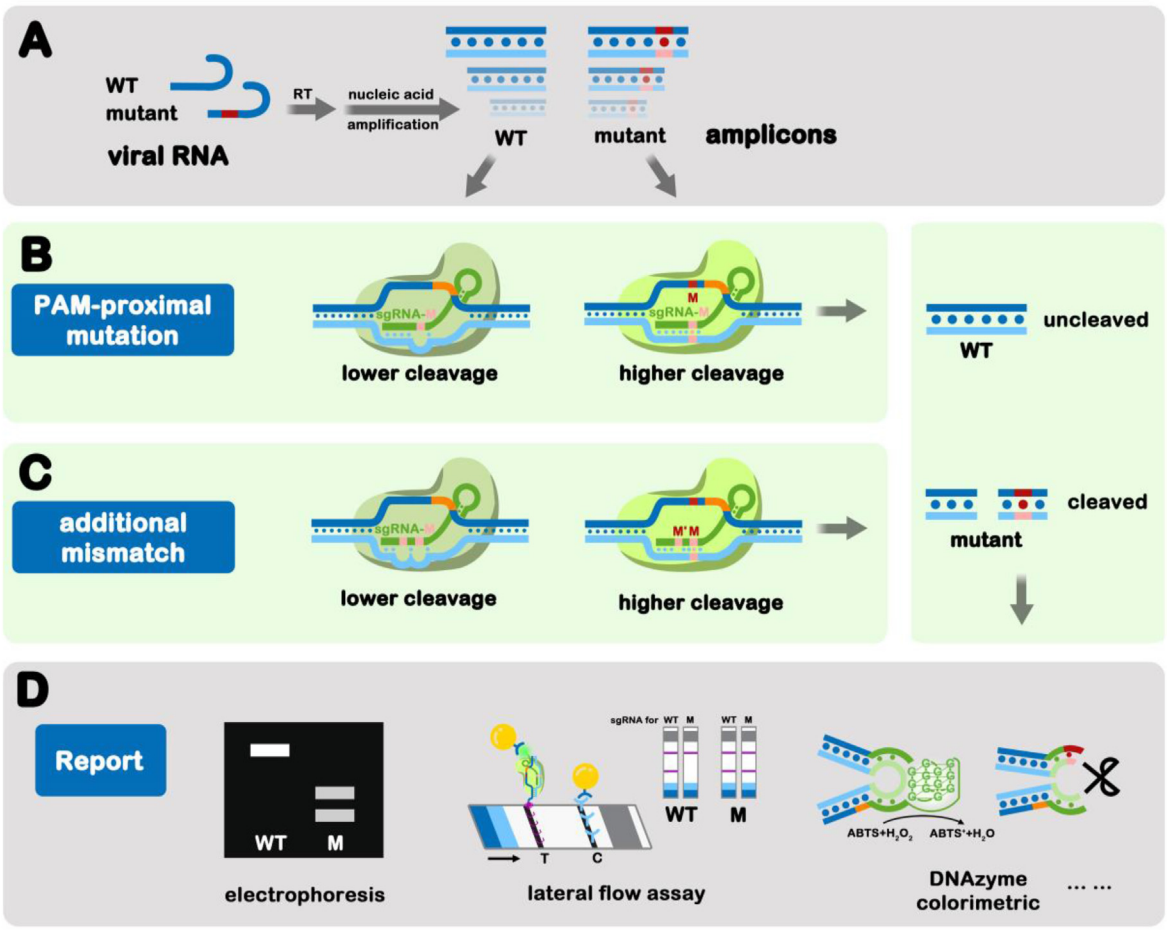

Fig. 3. Assays incorporating CRISPR-Cas9 for the detection of SARS-CoV-2 variants. **A.** Viral RNA was first reverse transcribed (RT) and amplified to amplicons of the wild-type (WT) and mutant sequences. **B**–**C.** The sgRNA-Cas9 ribonucleoprotein preferentially binds to the amplicons of the mutant sequence. Two strategies were used to increase the specificity of the Cas9 system for the mutant sequence. **B.** Selecting mutation sites located in the PAM-proximal region. **C.** Including additional mismatch to the spacer of sgRNA. **D.** Several biosensing methods were incorporated to convert Cas9 cleavage products to readable signals. Electrophoresis, lateral flow assays, and DNAzyme-based colorimetric assays are shown as examples.

mutations located in the PAM-proximal region (Fig. 3B) and introducing additional mismatches between the spacer sequence of sgRNA and the target (Fig. 3C). Both strategies used sgRNA designed to recognize the specific mutation target of a variant. Ideally, this sgRNA would not bind with the sequence of the original SARS-CoV-2 strain (the wild-type). The cleavage products formed by the amplicon-activated Cas9 system can be converted to readable signals using diverse reporter systems (Fig. 3D).

3.1. Designing crRNA to target mutations located in the PAM-proximal region for the Cas9-based detection of variants

Cas9 nucleases are more sensitive to PAM-proximal mismatches than to PAM distal mismatches [1,2,116]. Therefore, targeting mutations located in the PAM-proximal region (1–12 nt) facilitates the differentiation and detection of variants. Song et al. [123] reported a colorimetric assay for the differentiation and detection of SARS-CoV-2 and its variants. Three mutations, D614G, T478K, and A67V, were targeted for the detection of variants. For the detection of SARS-CoV-2, the viral RNA was amplified by RT-LAMP using primers containing G-quadruplex complementary sequences. Consequently, G-quadruplex sequences were embedded in the LAMP products. Because G-quadruplex complementary sequences were modified with phosphorothioate, the hybrid between the G-quadruplex and its complementary sequence is unstable. Therefore, G-quadruplex sequences dissociated from the hybrid and formed the G-quadruplex structure that further catalyzed the oxidation of ABTS (2,2′-azino-bis(3-ethylbenzothiazoline-6-sulfonic acid)) by hydrogen peroxide, generating a colorimetric signal for detection. Three pairs of sgRNAs, each containing a mutation-specific sgRNA and a wild-type-specific sgRNA, were then designed to guide Cas9 nucleases to target three pairs of the mutant and wild-type sequences, respectively. These sgRNAs guided the Cas9 protein to generate a double-strand break within the G-quadruplex domain. Breakage of the G-quadruplex diminished the catalytic reaction needed for color generation. For the detection of variants, triplicate RT-LAMP reactions were conducted for each sample. The colorimetric signals were observed from all the samples containing either wild-type SARS-CoV-2 or its variants. For differentiation of the wild-type from a specific variant, such as Omicron, the CRISPR-Cas9 reactions containing Omicron-specific sgRNA or wild-type-specific sgRNA were then applied to the second or third replicate of RT-LAMP reactions. In the presence of the Omicron variant, a decreased colorimetric signal was observed from the second replicate, while the third replicate showed a decreased colorimetric signal in the presence of the original strain. These decreases in colorimetric signals were used to identify and detect specific variants. D614G was detected in all variants, A67V was detected in the

Omicron variant, and T478K was detected in the Delta variant. These mutations are present in the PAM-proximal region (1–12 nt), which is favorable for the specificity of the detection of these variants.

3.2. Introducing additional mismatches into the spacer of Cas9 sgRNA to improve the specificity

The detected regions of sequences of variants often differ by a single nucleotide. Therefore, two DNA targets with only a single nucleotide difference must be discriminated. However, the specificity of CRISPR-Cas9 systems is often insufficient to achieve highly specific detection of a single mismatch. Introducing an additional mismatch into the spacer of sgRNA has been demonstrated to be an effective strategy for improving the specificity of CRISPR-Cas9 systems [116]. With two mismatches between the spacer and the wild-type gene, the undesired cleavage of the wild-type gene is significantly reduced. However, the additional mismatch also impairs the desired cleavage of the variant sequence. Thus, for good discrimination, the optimization of the site when introducing an additional mismatch is often required.

Kumar et al. [103] used this two-mismatch strategy to detect the N501Y mutation. The viral RNA was first amplified by RT-PCR and a sgRNA containing an additional mismatch was used to probe the amplicons containing the N501Y mutation. The additional mismatch was introduced at the 6th nt upstream to PAM and the N501Y mutation was located at the 2nd nt. A biotin-labeled primer and FAM-labeled sgRNA were used to allow the FAM, biotin-labeled RNP-amplicon complex to be captured by a streptavidin-coated strip, achieving a paper strip detection. Compared to the results from the deep sequencing on 37 wild-type and 22 N501Y-containing variant samples, a sensitivity of 87% and specificity of 97% were achieved in the detection of the N501Y mutation. A similar design was also applied to the detection of the E484K and T716I mutation targets [103].

4. CRISPR-Cas12-based methods for the detection of variants

The Cas12 family, including Cas12a, Cas12b, Cas12f (also called Cas14), and other subtypes, target both ssDNA and dsDNA using the crRNA guide [6,26,28,124]. Among these Cas12 proteins, Cas12a is most widely used in CRISPR-based diagnostic methods. Cas12a has a bilobed architecture: an N-terminal recognition lobe (REC) is linked by the wedge (WED) domain to a C-terminal nuclease lobe (NUC) [125]. The NUC lobe consists of PAM-interacting (PI), bridge helix (BH), RuvC, and Nuc domains [125]. The REC lobe takes charge of crRNA binding. Following the pre-order of the crRNA seed segment, two lysines in WED and PI domains recognize the PAM sequence (canonical 5′-TTTV-3′) and insert into the backbone of dsDNA, leading to the unwinding of the dsDNA [9,126]. As a result, the spacer of the crRNA hybridizes with the target strand in the dsDNA, together with the non-target strand, forming an R-loop structure. The stability of the R-loop is the key factor of Cas12a targeting specificity, and is affected by the mismatch between crRNA and the target strand [125,127]. The formation of the R-loop, including the target recognition and binding, leads to the rearrangement of the REC lobe of Cas12a, unlocking the catalytic site in the RuvC domain [125]. This catalytic site then cleaves both the non-target strand and the target strand in order, generating a staggered double-strand break [9]. In addition to its nuclease activity often called *cis*-cleavage activity that specifically cleaves target DNA, Cas12a also exhibits *trans*-cleavage activity that can nonspecifically cleave the ssDNA substrate [27]. The *trans*-cleavage of Cas12a is a multiple turnover process, which is useful for signal amplification [128].

Cas12a has a higher tolerance for mismatches and a lower specificity when ssDNA is the target compared to the dsDNA target [27,129]. Cas12a is highly sensitive to mismatches in the PAM region, because PAM recognition via both its shape and base-dependent mechanism is the first step before target binding [126]. Mismatches in the PAM-proximal region, especially in the seed segment (position 1st – 6th nt) of crRNA, are less tolerated by Cas12a [9]. Accordingly, several crRNA modification strategies have demonstrated effectiveness in increasing the specificity of CRISPR-Cas12a. The main modifications of crRNA included introducing an additional mismatch to the spacer [130,131], engineering a secondary structure onto the spacer [122], and using DNA chimeric crRNA [132]). The use of different Cas12 proteins and specific Cas12a homologs may also benefit the specificity [133].

Assays incorporating CRISPR-Cas12a for the detection of SARS-CoV-2 variants often use reporter probes dually labeled with a fluorophore and a quencher. The *trans*-cleavage activity of Cas12a facilitates the cleavage of reporter probes and generates amplified signals. The sensitivity of these assays is further improved by integrating CRISPR-Cas12a with nucleic acid amplification techniques, including PCR [134–137], RPA [27,107,138], and LAMP [34,139]. The viral RNA is reverse transcribed, the complementary DNA is amplified, and the amplicons are subsequently detected (Fig. 4A). Three main strategies have been used to improve the specificity of the detection: using the mutation site to act as the PAM domain for Cas12a targeting (Fig. 4B), targeting mutations located in the PAM-proximal region (Fig. 4C), and introducing additional mismatches into the spacer of crRNA (Fig. 4D).

4.1. Using the mutation site to act as the PAM domain for Cas12a targeting

A canonical PAM domain (5′-TTTV-3′) is essential to the target recognition of the CRISPR-Cas12a system. If a mutation site coincidentally has the same sequence as the PAM, the use of the mutation site to act as the PAM allows the Cas12a to specifically differentiate the mutation site from its wild-type sequence because the wild-type does not share the PAM sequence and is not favorable to the target recognition of Cas12a. This strategy has been used to develop CRISPR-Cas12a-based methods for the detection of SARS-CoV-2 variants. For example, Marqués et al. [135] developed a CRISPR-Cas12a-based assay for the detection of the E484K mutation. The E484K mutation, first identified in the Beta and Gamma variants, is a substitution of guanine by adenine in the S gene, leading to three consecutive adenines (WT 5′-TGAA-3′ and mutant 5′-TAAA-3′), which forms a canonical PAM sequence on the antisense strand (WT 5′-TTCA-3′ and mutant 5′-TTTA-3′). Therefore, this mutant sequence on the antisense strand 5′-TTTA-3′ was used to act as the PAM, and the corresponding crRNA was designed to target the sequence downstream of the PAM. Interestingly, about only a 2–fold signal intensity difference was observed for the detection of E484K mutation and the wild-type sequence at the same concentration. This small difference may be attributed to the tolerance of the CRISPR-Cas12a system to the sub-optimal PAM. Because E484K is not a variant-specific mutation, this assay cannot be used to differentiate specific variants. To achieve the differentiation of specific variants, Ning et al. [107] developed a CRISPR-Cas12a-based method for the detection of the Alpha and Delta variants. The Alpha variant has a unique mutation S982A, which corresponds to the change of a canonical PAM sequence in the WT (5′-TTTC-3′) to a non-canonical PAM sequence in the mutant (5′-TTGC-3′). The Delta variant has a specific mutation D950N (WT 5′-CAAG-3′ and mutant 5′-CAAA-3′). This mutation creates a canonical PAM on the antisense strand (WT antisense strand 5′-CTTG-3, and mutation antisense strand 5′-TTTG-3′). Thus, Ning et al. [107] chose

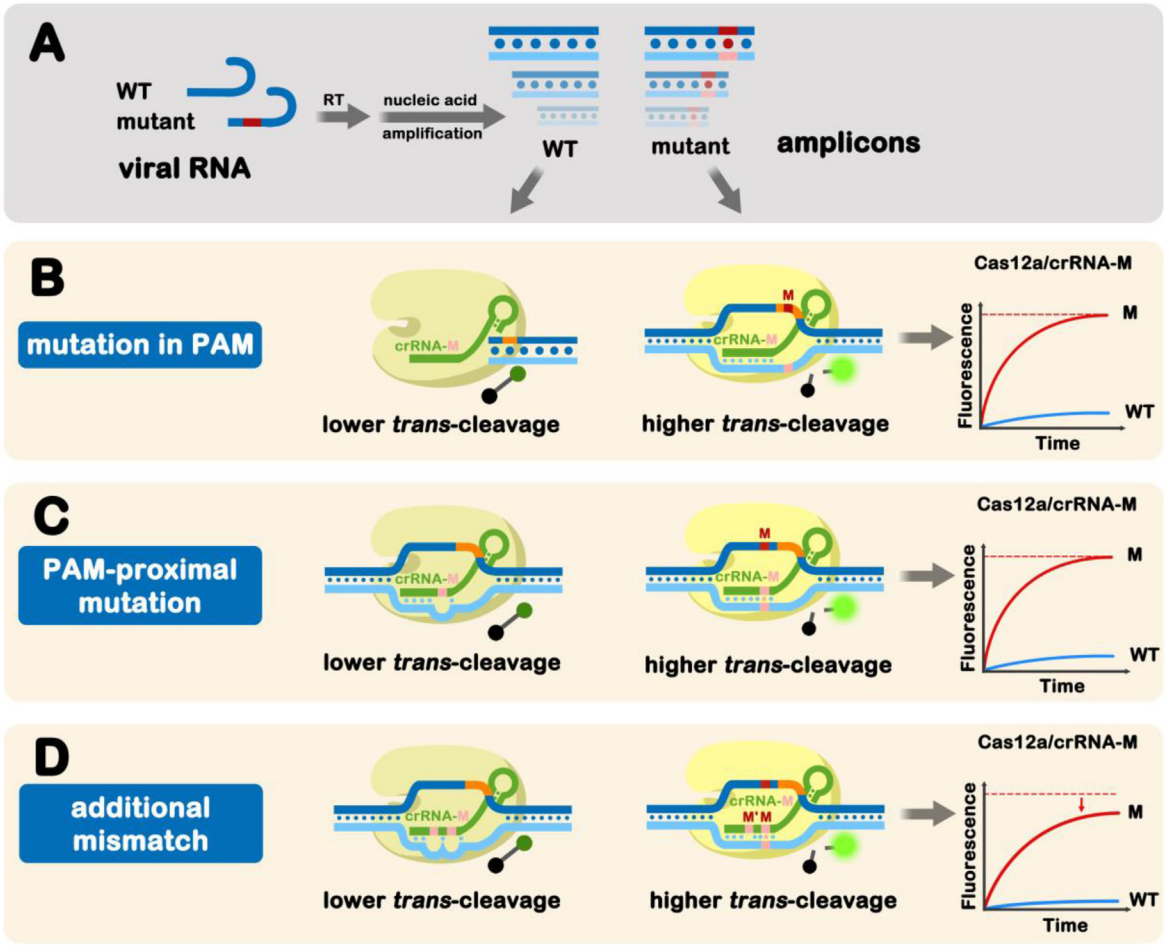

Fig. 4. Assays incorporating CRISPR-Cas12a for the detection of SARS-CoV-2 variants. **A.** Viral RNA was first reverse transcribed (RT) and amplified to amplicons of WT or mutant sequence. **B**–**D**. The Cas12a-crRNA RNP preferentially binds to the amplicons of the mutant sequence. Three strategies were used to increase the specificity of the Cas12a system for the mutant sequence. **B.** Choosing mutation sites to act as PAM sequence. **C.** Targeting mutation site located in the PAM-proximal region. **D.** Including an additional mismatch to the crRNA spacer. The crRNA designed for the specific variant sequence (crRNA-M) preferentially recognizes and binds to mutation-containing amplicons but not (or minimally) to the WT amplicons. The mutation-containing amplicons activate the RNP, whose *trans*-cleavage activities generate detection signals from reporters, such as fluorescence.

these regions to serve as the PAM domain in their assay for these two variants. They observed about a 2.5- fold difference in the fluorescent signal between the target variant and non-target variants. They analyzed 16 Alpha positive nasal swab samples and 44 Delta-infected samples. The diagnostic sensitivity and specificity were 88.2% and 92.6% for the detection of the Alpha variant, and 97.6% and 94.8% for the Delta variant.

Although using the mutation site to act as PAM has been demonstrated to enable differentiation and detection of SARS-CoV-2 variants, two issues limit its wide application: the strategy only applies to mutations capable of serving as the PAM domain and the tolerance of the CRISPR-Cas12a towards the sub-optimal PAM sequence compromises the detection specificity.

4.2. Targeting mutations located in the PAM-proximal region for Cas12-based detection of variants

Like CRISPR-Cas9 systems, the CRISPR-Cas12a system also has various sensitivities to mismatches located in different protospacer regions. Studies have shown that the CRISPR-Cas12a is less tolerant of mismatches located in the PAM-proximal region than of those in the PAM-distal region, because mismatches in the PAM-proximal region have a stronger effect on the stability of the R-loop [127]. Therefore, targeting mutations located in the PAM-proximal region is useful for Cas12a to recognize the specific target. Single-nucleotide mismatches within the first six bases proximal to PAM significantly impacted the *trans*-cleavage activity of Cas12a [27]. On the basis of this finding, Liang et al. [136] developed a CRISPR-Cas12a-mediated mutation-specific assay and detected six mutations in a total of 59 clinical samples involving the wild-type and four major variants. In their design of crRNA, the authors considered targeting six mutations, E484K, K417N, L452R, T478K, N501Y, and D614G, for the differentiation of the four variants. The E484K mutation was located at the PAM site on the antisense strand. N501Y and D614G mutations had a canonical PAM sequence (5′-TTTV-3′) upstream of the mutation site. The three mutation sites (K417N, L452R, and T478K) did not contain an upstream PAM sequence. Therefore, the authors designed PCR primers to insert a PAM sequence into the non-target strand of the amplicons. To ensure specificity, the authors kept all the mutation sites within 10 bp proximal to PAM. In comparison with the results of the DNA sequencing, this assay achieved 83.3–100% positive prediction and 85.7–100% negative prediction. The approach of selecting mutations located in the PAM-proximal region has also been exploited to develop other assays for the differentiation and detection of SARS-CoV-2 and its variants [102,137–140]. In these assays, CRISPR-

Cas12a-mediated detection was combined with other isothermal amplification techniques such as RPA and LAMP and with various detection methods such as surface plasmon resonance (SPR) and LED light-based visual/cellphone detection [102,137–140].

Although targeting mutations located in the PAM-proximal region has improved the specificity of CRISPR-Cas12a for the differentiation of SARS-CoV-2 and its variants, the ability of CRISPR-Cas12a to differentiate single nucleotide polymorphisms (SNPs) still needs to be further improved. A single-nucleotide mutation does not always lead to a decrease in the signal at a particular time point [141]. In a test covering all 60 possible mutations within a 20 nt protospacer, the mutant even had a higher signal than the wild-type at one time point [141]. An alternative strategy was to use the kinetics parameters for variant discrimination, because all these variants exhibited a lower apparent catalytic efficiency (k^*_{cat}/K_M) than that of the wild-type [141].

4.3. Introducing additional mismatches into the spacer of crRNA to improve the specificity of CRISPR-Cas12a-based detection

It is often challenging for CRISPR-Cas12a to specifically differentiate a single mismatch. Introducing an additional mismatch into the spacer of crRNA can improve the specificity of the CRISPR-Cas12a system. Compared to a single mismatch, two mismatches can significantly reduce the stability of the R-loop, thereby decreasing the *trans*-cleavage activity of Cas12a. Additionally, the location of the additional mismatch can be rationally designed, so that the impact of this mismatch on the *trans*-cleavage activity of Cas12a can be tuned. He et al. [142] reported a CRISPR-Cas12a-based mutation detection method by adding an additional mismatch into the spacer of crRNAs for the detection of mutations N501Y and D614G. The mutation site was located at the 10th nt for N501Y and the 6th nt for D614G downstream of the selected 5′-TTTV-3′ PAM sequence. An additional mismatch was introduced at the 3rd nt for N501Y and the 4th nt for D614G into the spacer of crRNA for both the wild-type and the mutant. The authors achieved good discrimination between the wild-type and the mutant and observed 100% consistency of results compared to those of the DNA sequencing for the detection of 18 clinical variant samples. Similarly, Huang et al. [104] also introduced an additional mismatch to crRNA to detect the mutation D614G. The additional mismatch was introduced at various sites of the spacer of the crRNA from −3 to +3 site around the mutation site. The site (−1) showed the best discrimination and this design was used for the detection of D614G. The approach was also used for the detection of other mutations through the combination of CRISPR-Cas12a-mediated detection with isothermal amplification techniques, including RPA, LAMP, and isothermal recombinase-aided amplification [105,143,144].

Instead of introducing an additional mismatch, Liang et al. [145] considered three adjacent mutations and designed a single crRNA to probe the target containing these mutations. They designed one crRNA designed for sensing the S371L, S373P, and S375F mutations, and another for the Q493R, G496S, and Q498R mutations. Although CRISPR-Cas12a can efficiently differentiate the wild-type from the variant by examining the presence of three mutations, not many relevant targets contain three adjacent mutations. In another strategy, Yang et al. [106] replaced 8 nt of crRNA with DNA and used this chimeric crRNA to recognize the N501Y mutation. The chimeric crRNA increased the specificity of Cas12a by affecting the hybridization energy and inducing instability in off-target DNA binding [106].

4.4. Assays using other types of Cas12 proteins

Besides Cas12a, other types of Cas12 proteins have been used for the detection of variants of SARS-CoV-2 because of their better thermal stability or their higher specificity. Nguyen et al. [139] reported a one-pot assay that combined RT-LAMP with CRISPR-BrCas12b for the detection of SARS-CoV-2 variants. This method achieved one-pot discrimination of the five VOCs through the precise design of RT-LAMP primers and crRNA. The BrCas12b protein remains stable and has high activity at 60–65 °C, so it is compatible with the RT-LAMP reaction. Another homolog, Cas12f (also known as Cas14), shows a better specificity for the detection of SNPs [124]. However, Cas12f has not been used for the detection of SARS-CoV-2 variants. Fasching et al. [146] compared a newly identified Cas12 protein CasDx1 with two other homologs, LbCas12a and AsCas12a, for their SNP discrimination ability. They tested multiple mutations, L452R, E484K/Q/A, and N501Y. CasDx1 showed the best specificity for the detection of these mutations.

5. CRISPR-Cas13-based methods for detection of variants

There are several distinct features between CRISPR-Cas13 and CRISPR-Cas12 although they both possess *trans*-cleavage and *cis*-cleavage activities [19,28,29]. First, the activators of CRISPR-Cas12 are DNA [26,27], whereas the activators of CRISPR-Cas13 are ssRNA [29]. Second, target recognition of the CRISPR-Cas12 requires the presence of a PAM domain adjacent to the target DNA [9,26], whereas the target recognition of CRISPR-Cas13 generally prefers a protospacer flanking site (PFS), a non-G nucleotide site, on the 3′-end of the ssRNA target [29]. Third, the *trans*-cleavage activity of the CRISPR-Cas12 cleaves ssDNA substrates, whereas the *trans*-cleavage activity of the CRISPR-Cas13 non-specifically cleaves ssRNA substrates [19]. The *trans*-cleavage activity of the CRISPR-Cas13 also exhibits a high turnover number, which has been used for amplified detection of SARS-CoV-2 and its variants. The CRISPR-Cas13 family includes four subtypes, Cas13a, Cas13b, Cas13c, and Cas13d [29,147–149]. Among these subtypes, Cas13a is most widely used for the detection of nucleic acids [30,150–154].

The specificity of CRISPR-Cas13a nucleases relies on the specific binding of the target RNA with the crRNA and the subsequent activation of the nuclease. The binding of the target RNA triggers a large conformation change of the Cas13a protein, bringing the two halves of the HEPN (higher eukaryotes and prokaryotes nucleotide) binding domain active site into proximity and forming an active nuclease site on the external surface [10,155]. The nuclease site then begins to cleave the target RNA and nonspecific ssRNA [10,155]. Efforts to improve the specificity of Cas13a have been mainly focused on the design and engineering of crRNA, including truncating the spacer of crRNA [30,150], introducing additional mismatches into the spacer of crRNA [30,152,153,156], modulating the secondary structure of crRNA [157], and using algorithms to design highly specific crRNA [158]. The second and fourth approaches have been exploited to develop CRISPR-Cas13-based methods for the differentiation and detection of SARS-CoV-2 and its variants.

CRISPR-Cas13a facilitates the highly specific detection of SARS-CoV-2 variants through amplification-free detection [159] or together with nucleic acid amplification techniques, including RT-PCR and RT-RPA (Fig. 5 A) [101,108,160–162]. Compared with CRISPR-Cas9-based and CRISPR-Cas12-based assays that detect the dsDNA amplicons directly, the CRISPR-Cas13-based assay requires a T7-transcription step to transcribe the amplified DNA target into the corresponding RNA because the CRISPR-Cas13 system can only be activated by RNA targets [29].

5.1. Optimizing the mismatch location in the spacer of the crRNA to improve the specificity of CRISPR-Cas13-based detection

The number and location of mismatches present in the spacer of crRNA have an impact on the binding of crRNA to the target RNA

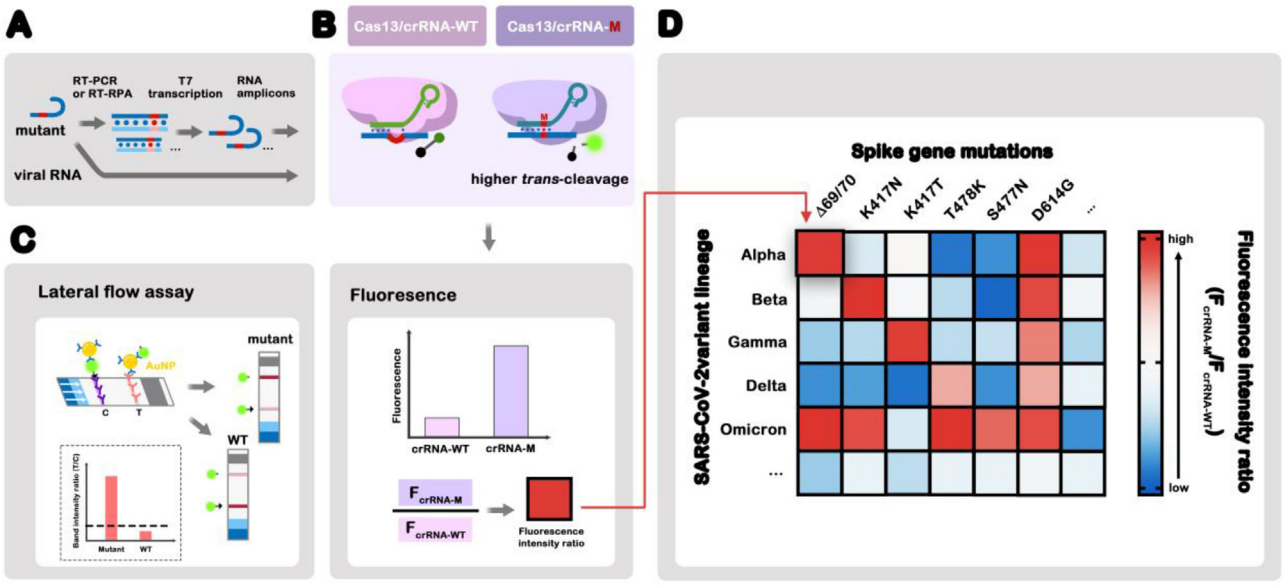

Fig. 5. Discrimination of SARS-CoV-2 variants using CRISPR-Cas13. **A.** Viral RNA can be analyzed directly. DNA or amplicons of RT-PCR and RT-RPA must be transcribed to RNA using T7 transcription. **B.** A typical crRNA pair (Cas13/crRNA-WT for the original sequence and Cas13/crRNA-M for the mutant sequence) is used for the discrimination of the wild-type and the mutant. **C.** Examples of lateral flow assay and fluorescence detection of the wild-type (WT) and mutants. In the lateral flow assay, a ratio of higher signal intensity of the test line over that of the control line denotes the presence of the variant. In the fluorescence test, a higher fluorescence signal in the crRNA-M assay than that in the crRNA-WT assay denotes a mutant. **D.** Discrimination of specific variants using the results of fluorescence detection of variant-specific mutation sites in the S gene. For each mutation site, the ratio of the fluorescence intensity from the crRNA-M assay to that of the crRNA-WT assay was measured. A fluorescence intensity ratio higher than a certain threshold (red squares) indicates the presence of a mutation site.

and nuclease activiy of LbuCas13a [163]. The mismatches in the middle region (9–12 nt) from the 5'-end of the spacer of crRNA have a larger impact on the binding affinity between RNP and the target than those in other locations, and mutations in the 5–8 nt region have a greater impact on the nuclease activity [163]. Therefore, optimizing the mismatch location to the spacer of the crRNA is of great importance for the specificity of the CRISPR-Cas13a. Shinoda et al. [159] reported a LtrCas13a-based amplification-free assay for the discrimination of SARS-CoV-2 variants. They designed pairs of crRNA, with one crRNA specific for the wild-type target and the other crRNA recognizing the mutation target (Fig. 5B). When designing these crRNA pairs, they placed the mismatches in the spacer region of 1–10 nt to target the mutations N501Y, E484K, and L452R, and examined the location of mismatches to achieve specific detection. They used each pair of crRNAs to conduct two assays for each sample. The signal intensity ratio between the two assays, one using the mutation-specific crRNA and the other using the crRNA for the wild-type, provided information for the differentiation of the wild-type from the mutant targets. Their results showed that the optimized location of a mismatch for each crRNA pair was 7/7 for N501/Y501, 5/5 for E484/K484, and 7/8 for L452/R452 [159]. These results were consistent with the previous observation that mismatches in the 5–8 nt had a larger impact on the nuclease activities of Cas13 [163]. Shinoda et al. [159] examined the specificity of the method by analyzing 60 whole genome sequencing-verified clinical samples: 10 B.1.1.214/284, 10 Alpha, 10 R.1 (a variant with 501 N and 484K), 10 Delta, 10 Omicron, and 10 negative samples. A 98% specificity was obtained for the discrimination of these variants [159]. Although the method does not involve target amplification, the need for sophisticated equipment limits its applications.

5.2. Introducing additional mismatches into the spacer of crRNA to improve the specificity of CRISPR-Cas13-based detection

LwaCas13a can detect SNPs with a crRNA containing a synthetic mismatch [30]. The highest specificity was obtained when the mutation was present at the 3rd nt and a synthetic mismatch was at the 5th nt of the spacer from the 5′-end of crRNA [30]. Introducing synthetic mismatches into the spacer of crRNA was also used to improve the specificity of CRISPR-Cas13 for the detection of SARS-CoV-2 variants. Casati et al. [162] added two or three synthetic mismatches into the spacer of the crRNAs for specific discrimination of variants. Mutations D80A and T478K were selected for the detection of Beta and Delta variants, and two synthetic mismatches were added into the crRNA for each mutation site. The crRNA for Alpha variant detection was completely complementary to the region covering the wild-type 67A and HV69-70 deletion of the Alpha variant. Three synthetic mismatches were introduced into Omicron-targeting crRNAs covering the HV69-70 deletion and A67V mutation of Omicron variants. Lateral flow strips were used to visualize the amount of FAM reporters cleaved by Cas13a. Although each crRNA was designed to detect one specific variant, non-target variants also generated visible test lines. Thus, whether a specific variant was present could not be determined by the presence or absence of a band at the test line. To solve this issue, the authors used the ratio of the band intensity of the test line to that of the control line to determine whether a sample contained a specific variant (Fig. 5C). This approach reduced the variability of the loaded sample volume. A threshold was then set to interpret the results and determine the presence of a specific variant. A total of 20 variant samples (five for each variant) were tested and 100% specificity was reported although the number of the tested samples was small [162].

5.3. Using algorithms to help design the crRNA of CRISPR-Cas13 with high specificity

Algorithms have been used to design crRNAs with high specificity to complement experimental optimization [108,158,161]. Welch et al. [161] used a generative sequence design algorithm based on a machine learning system (called ADAPT [158]) to design crRNA of Cas13a with estimated maximal on-target and minimal off-target activity. Twenty-six crRNA pairs were then designed to differentiate the wild-type and 26 specific mutations on the S gene, which were shared by or were unique for Alpha, Beta, Gamma, Delta, and Epsilon variants. The performance of these 26 crRNA pairs was then tested with synthetic RNA and validated with RNA extract from viral seed stock (wild-type or the five variants). Each sample was first amplified using RT-PCR, followed by T7 transcription. A multi-testing microfluidic platform was then used to test RNA products of T7 transcription, and each sample was tested with these 26 crRNA pairs. The $\log_2$ ratio of the fluorescence from the mutation-specific crRNA to that of the wild-type specific crRNA was used to determine the presence of a specific variant. The variant specimens, 24 Alpha, 23 Beta, 24 Gamma, 6 Delta, and 24 Epsilon, were tested and a 97% specificity was obtained in comparison with outcomes from next-generation sequencing (NGS).

The same algorithm was also used to design crRNA for the discrimination of SNPs in a Cas13a-mediated RPA assay [108]. Three crRNAs were designed to discriminate Beta and Gamma variants from the wild-type with only one nucleotide difference (N417, T417, K417). The combination of algorithms with rational engineering of crRNA is anticipated to further improve the design of crRNA with high performance.

5.4. Using signal intensity ratios to achieve discrimination of variants

Single-nucleotide resolution is often required for the differentiation and detection of SARS-CoV-2 and its variants. Although discrimination of SARS-CoV-2 variants has been achieved through different strategies for improving the specificity of CRISPR-Cas13, detection signals are often observed from the detection of non-target variants with crRNA of the target variants. Therefore, the presence of the detection signal cannot be used to determine whether the test is positive or negative for a specific variant. To solve this issue, researchers used signal ratios to interpret the results and assist in the discrimination of the variants (Fig. 5C−5D).

The signal ratios were generally calculated based on detection signals from using a pair of crRNAs, mutation-specific crRNA, and wild-type specific crRNA. For instance, Welch et al. [161] conducted Cas13a-based detection for each sample by using mutation-specific and wild-type specific crRNAs and then calculated the $\log_2$ signal ratios of the fluorescence signal of mutation-specific crRNA to wild-type specific crRNA or the reverse ratios. This signal ratio represented the difference in the sensitivity of these two crRNAs for the detection of the same sample, and therefore is independent of target concentrations. A threshold was established based on the results of testing of wild-type and variant control samples. The comparison of signal ratios with the threshold value was used to determine the presence or absence of specific variants. Alternatively, Arizti-Sanz et al. [108] used the ratio of background-subtracted fluorescence signal from a wild-type specific/mutation-specific crRNA to the highest signal in the same batch of testing, which could reduce variations from the use of different crRNA and detection process.

6. Concluding remarks and future perspectives

Cas9, Cas12, and Cas13 nucleases have been used to develop CRISPR-based methods for the detection and differentiation of SARS-CoV-2 VOCs. These methods generally used nucleic acid amplification techniques, including PCR and isothermal amplification techniques, to first amplify selected viral RNA regions that contain mutations characterizing specific variants. Specific crRNAs were designed and used together with Cas nucleases to recognize and differentiate amplicons containing the mutations. Various signal responses were generated from Cas nuclease activities, achieving sensitive detection. Different combinations of nucleic acid amplification techniques with crRNA and Cas nucleases led to differences in the specificity, sensitivity, and applicability of CRISPR-based methods.

We compared three main types of Cas proteins, Cas9, Cas12, and Cas13, that have been used for the differentiation and detection of SARS-CoV-2 variants. We discussed their advantages and limitations (Table S4). Cas12 and Cas13 have multiple turnover *trans*-cleavage activity in addition to *cis*-cleavage of the target. Cas9 has *cis*-cleavage activity only, which is single-turnover. The multiple turnovers of *trans*-cleavage provide additional amplification ability of Cas12 and Cas13 compared to the Cas9 system, facilitating signal generation and signal amplification.

The specificity of these CRISPR-based methods relies on the capability of the CRISPR-Cas systems to differentiate mutant sequences from the wild-type sequence and to differentiate mutations among variants. The differentiation of nucleic acid strands containing a single-nucleotide mutation is technically challenging. Therefore, it is critical to improve the specificity of CRISPR-Cas systems for the specific detection of SARS-CoV-2 variants.

Typical CRISPR-Cas9, -Cas12, and -Cas13 systems are each composed of two main elements, a Cas nuclease and a guide RNA (sgRNA for Cas9 or crRNA for Cas12 and Cas13). The guide RNA recognizes the specific nucleic acid target and guides the Cas protein to bind to the target. The target binding activates the nuclease activity of the Cas protein. In principle, improvements in specificity can be achieved by engineering the Cas protein with higher specificity and modifying the guide RNA for specific interactions. Because engineering the Cas protein is more laborious and less predictable, most approaches used for improving the specificity of CRISPR-Cas systems focused on the crRNA.

Much research on the design of guide RNA for specific CRISPR-based assays has been built on previous findings about the specificity of CRISPR-Cas systems. Thus, guide RNA design strategies have considered the importance of the PAM site for the RNA-guided target recognition of Cas9 and Cas12 and differences in the Cas response to mismatches on different sites of the spacer-binding region. PAM-free CRISPR-Cas systems have been discovered through protein engineering and natural Cas ortholog mining [164,165]. These PAM-free CRISPR-Cas systems provide more flexibility in the selection of target sites. However, the decreased requirement for PAM can increase the likelihood of off-targeting, compromising the specificity of CRISPR-Cas systems [165]. No PAM-free Cas proteins have been used to detect SARS-CoV-2 and its variants.

Because CRISPR-Cas systems exhibit different tolerance to the position of mismatches, the mismatch position is an important optimizing parameter for achieving high specificity. For Cas9 and Cas12 that require a PAM site for target binding, mismatches in the PAM proximal region are less tolerated than those in the PAM distal region. Targeting mutations located in the PAM-proximal region is an effective strategy for improving the specificity of the Cas9- and

Cas12-based methods. Cas13a does not require a PAM site, and the position of the target mutation is less important for specificity. Additional approaches of engineering crRNA to improve the specificity of CRISPR-Cas systems include truncating the spacer of crRNA, introducing modified nucleotides into the spacer of crRNA, and changing a nucleotide in the spacer of the crRNA to create an additional mismatch with the target.

The improved design and modification of crRNA using several approaches have enabled CRISPR-based techniques to detect and differentiate specific SARS-CoV-2 variants. Some studies have reported a discrimination factor higher than 50 between the mutant and wild-type sequences. Although higher detection signals were generated from the analysis of the specific mutation sequence, lower but non-negligible signals generated by the wild-type sequence remained a problem in real-world clinical diagnostics. The viral load and concentrations of SARS-CoV-2 RNA in clinical samples could vary by more than four orders of magnitude. The discrimination factor of 50 is not sufficient to differentiate mutations from the wild-type sequence at diverse concentrations. Therefore, these techniques are not adequate for the clinical diagnosis of specific SARS-CoV-2 variants.

To deal with the issue of concentration differences, researchers used the ratio of the signal intensities generated from the analysis of the same sample using the methods with two crRNAs. One crRNA was designed to recognize a specific mutation in the variant and the other crRNA was designed to recognize a conservative region of the viral RNA. The signal intensity ratio was independent of the concentration of the RNA sample and improved the identification of specific variants. This approach required analyses of the same sample twice using two methods: one with crRNA recognizing the wild-type sequence and the other with crRNA recognizing the mutant sequence.

The potential of point-of-care testing is one of the main reasons for using Cas nucleases to generate easily detectable signals. However, current CRISPR-based methods developed for the detection of SARS-CoV-2 variants involve multiple steps, which are not friendly to point-of-care testing. The Cas13a system has been used to directly differentiate and detect specific SARS-CoV-2 RNA sequences without the need for other amplification. The potential of this system could be further exploited and could lead to simpler and rapid assays for point-of-care testing of SARS-CoV-2 variants. With the emergence of different sublineages of variants, new techniques are also needed to discriminate among the sublineages in addition to identifying different variants.

Declaration of competing interest

The authors declare that they have no known competing financial interests or personal relationships that could have appeared to influence the work reported in this paper.

Data availability

Data will be made available on request.

Acknowledgments

This work was supported by the New Frontiers in Research Fund, the Natural Sciences and Engineering Research Council of Canada (NSERC), the Canadian Institutes of Health Research (CIHR), the Social Sciences and Humanities Research Council of Canada (SSHRC), the Canada Research Chairs program, Alberta Innovates, and Alberta Health. H.X. and W.F. acknowledge scholarship support from the Chinese Scholarship Council. J.T. acknowledges the support of an NSERC Postgraduate Doctoral Scholarship (PGS-D). J.X. acknowledges the support of an NSERC Alexander Graham Bell Canada Graduate Scholarship (CGS-D). T.K. acknowledges the support of an Alberta Graduate Excellence Scholarship and a Faculty of Medicine & Dentistry Dean's Doctoral Student Award from the University of Alberta.

Appendix A. Supplementary data

Supplementary data to this article can be found online at https://doi.org/10.1016/j.trac.2023.117000.

References

[1] M. Jinek, K. Chylinski, I. Fonfara, M. Hauer, J.A. Doudna, E. Charpentier, A programmable dual-RNA-guided DNA endonuclease in adaptive bacterial immunity, Science 337 (2012) 816–821. https://doi.org/10.1126/science.1225829.

[2] L. Cong, F.A. Ran, D. Cox, S. Lin, R. Barretto, N. Habib, P.D. Hsu, X. Wu, W. Jiang, L.A. Marraffini, F. Zhang, Multiplex genome engineering using CRISPR/Cas systems, Science 339 (2013) 819–823. https://doi.org/10.1126/science.1231143.

[3] B. Chen, L.A. Gilbert, B.A. Cimini, J. Schnitzbauer, W. Zhang, G.W. Li, J. Park, E.H. Blackburn, J.S. Weissman, L.S. Qi, B. Huang, Dynamic imaging of genomic loci in living human cells by an optimized CRISPR/Cas system, Cell 155 (2013) 1479–1491. https://doi.org/10.1016/j.cell.2013.12.001.

[4] W. Xue, S. Chen, H. Yin, T. Tammela, T. Papagiannakopoulos, N.S. Joshi, W. Cai, G. Yang, R. Bronson, D.G. Crowley, F. Zhang, D.G. Anderson, P.A. Sharp, T. Jacks, CRISPR-mediated direct mutation of cancer genes in the mouse liver, Nature 514 (2014) 380–384. https://doi.org/10.1038/nature13589.

[5] M. Adli, The CRISPR tool kit for genome editing and beyond, Nat. Commun. 9 (2018) 1911. https://doi.org/10.1038/s41467-018-04252-2.

[6] K.S. Makarova, Y.I. Wolf, J. Iranzo, S.A. Shmakov, O.S. Alkhnbashi, S.J.J. Brouns, E. Charpentier, D. Cheng, D.H. Haft, P. Horvath, S. Moineau, F.J.M. Mojica, D. Scott, S.A. Shah, V. Siksnys, M.P. Terns, Č. Venclovas, M.F. White, A.F. Yakunin, W. Yan, F. Zhang, R.A. Garrett, R. Backofen, J. van der Oost, R. Barrangou, E.V. Koonin, Evolutionary classification of CRISPR-Cas systems: a burst of class 2 and derived variants, Nat. Rev. Microbiol. 18 (2020) 67–83. https://doi.org/10.1038/s41579-019-0299-x.

[7] M. Jinek, F. Jiang, D.W. Taylor, S.H. Sternberg, E. Kaya, E. Ma, C. Anders, M. Hauer, K. Zhou, S. Lin, M. Kaplan, A.T. Iavarone, E. Charpentier, E. Nogales, J.A. Doudna, Structures of Cas9 endonucleases reveal RNA-mediated conformational activation, Science 343 (2014), 1247997. https://doi.org/10.1126/science.1247997.

[8] H. Nishimasu, F.A. Ran, P.D. Hsu, S. Konermann, S.I. Shehata, N. Dohmae, R. Ishitani, F. Zhang, O. Nureki, Crystal structure of Cas9 in complex with guide RNA and target DNA, Cell 156 (2014) 935–949. https://doi.org/10.1016/j.cell.2014.02.001.

[9] D.C. Swarts, J. van der Oost, M. Jinek, Structural basis for guide RNA processing and seed-dependent DNA targeting by CRISPR-Cas12a, Mol. Cell 66 (2017) 221–233. https://doi.org/10.1016/j.molcel.2017.03.016.

[10] L. Liu, X. Li, J. Ma, Z. Li, L. You, J. Wang, M. Wang, X. Zhang, Y. Wang, The molecular architecture for RNA-guided RNA cleavage by Cas13a, Cell 170 (2017) 714–726. https://doi.org/10.1016/j.cell.2017.06.050.

[11] G. Silva, L. Poirot, R. Galetto, J. Smith, G. Montoya, P. Duchateau, F. Paques, Meganucleases and other tools for targeted genome engineering: perspectives and challenges for gene therapy, Curr. Gene Ther. 11 (2011) 11–27. https://doi.org/10.2174/156652311794520111.

[12] F.D. Urnov, E.J. Rebar, M.C. Holmes, H.S. Zhang, P.D. Gregory, Genome editing with engineered zinc finger nucleases, Nat. Rev. Genet. 11 (2010) 636–646. https://doi.org/10.1038/nrg2842.

[13] J.K. Joung, J.D. Sander, TALENs: a widely applicable technology for targeted genome editing, Nat. Rev. Mol. Cell Biol. 14 (2013) 49–55. https://doi.org/10.1038/nrm3486.

[14] K. Pardee, A.A. Green, M.K. Takahashi, D. Braff, G. Lambert, J.W. Lee, T. Ferrante, D. Ma, N. Donghia, M. Fan, N.M. Daringer, I. Bosch, D.M. Dudley, D.H. O'Connor, L. Gehrke, J.J. Collins, Rapid, low-cost detection of zika virus using programmable biomolecular components, Cell 165 (2016) 1255–1266. https://doi.org/10.1016/j.cell.2016.04.059.

[15] W. Feng, A.M. Newbigging, J. Tao, Y. Cao, H. Peng, C. Le, J. Wu, B. Pang, J. Li, D.L. Tyrrell, H. Zhang, X.C. Le, CRISPR technology incorporating amplification strategies: molecular assays for nucleic acids, proteins, and small molecules, Chem. Sci. 12 (2021) 4683–4698. https://doi.org/10.1039/d0sc06973f.

[16] Y. Tang, L. Gao, W. Feng, C. Guo, Q. Yang, F. Li, X.C. Le, The CRISPR-Cas toolbox for analytical and diagnostic assay development, Chem. Soc. Rev. 50 (2021) 11844–11869. https://doi.org/10.1039/d1cs00098e.

[17] M.M. Kaminski, O.O. Abudayyeh, J.S. Gootenberg, F. Zhang, J.J. Collins, CRISPR-based diagnostics, Nat. Biomed. Eng. 5 (2021) 643–656. https://doi.org/10.1038/s41551-021-00760-7.

[18] R. Aman, A. Mahas, M. Mahfouz, Nucleic acid detection using CRISPR/Cas biosensing technologies, ACS Synth. Biol. 9 (2020) 1226–1233. https://doi.org/10.1021/acssynbio.9b00507.

[19] A. East-Seletsky, M.R. O'Connell, S.C. Knight, D. Burstein, J.H. Cate, R. Tjian, J.A. Doudna, Two distinct RNase activities of CRISPR-C2c2 enable guide-RNA processing and RNA detection, Nature 538 (2016) 270–273. https://doi.org/10.1038/nature19802.
[20] T. Zhang, W. Zhou, X. Lin, M.R. Khan, S. Deng, M. Zhou, G. He, C. Wu, R. Deng, Q. He, Light-up RNA aptamer signaling-CRISPR-Cas13a-based mix-and-read assays for profiling viable pathogenic bacteria, Biosens. Bioelectron. 176 (2021), 112906. https://doi.org/10.1016/j.bios.2020.112906.
[21] Y. Dai, R.A. Somoza, L. Wang, J.F. Welter, Y. Li, A.I. Caplan, C.C. Liu, Exploring the trans-cleavage activity of CRISPR-Cas12a (cpf1) for the development of a universal electrochemical biosensor, Angew. Chem. 131 (2019) 17560–17566. https://doi.org/10.1002/anie.201910772.
[22] D. Zhang, Y. Yan, H. Que, T. Yang, X. Cheng, S. Ding, X. Zhang, W. Cheng, CRISPR/Cas12a-mediated interfacial cleaving of hairpin DNA reporter for electrochemical nucleic acid sensing, ACS Sens. 5 (2020) 557–562. https://doi.org/10.1021/acssensors.9b02461.
[23] J.H. Choi, J. Lim, M. Shin, S.H. Paek, J.W. Choi, CRISPR-Cas12a-based nucleic acid amplification-free DNA biosensor via Au nanoparticle-assisted metal-enhanced fluorescence and colorimetric analysis, Nano Lett. 21 (2021) 693–699. https://doi.org/10.1021/acs.nanolett.0c04303.
[24] S. Gong, X. Wang, P. Zhou, W. Pan, N. Li, B. Tang, AND logic-gate-based CRISPR/Cas12a biosensing platform for the sensitive colorimetric detection of dual miRNAs, Anal. Chem. 94 (2022) 15839–15846. https://doi.org/10.1021/acs.analchem.2c03666.
[25] Y. Pang, Q. Li, C. Wang, S. Zhen, Z. Sun, R. Xiao, CRISPR-cas12a mediated SERS lateral flow assay for amplification-free detection of double-stranded DNA and single-base mutation, Chem. Eng. J. 429 (2022), 132109. https://doi.org/10.1016/j.cej.2021.132109.
[26] B. Zetsche, J.S. Gootenberg, O.O. Abudayyeh, I.M. Slaymaker, K.S. Makarova, P. Essletzbichler, S.E. Volz, J. Joung, J. van der Oost, A. Regev, E.V. Koonin, F. Zhang, Cpf1 is a single RNA-guided endonuclease of a class 2 CRISPR-Cas system, Cell 163 (2015) 759–771. https://doi.org/10.1016/j.cell.2015.09.038.
[27] J.S. Chen, E. Ma, L.B. Harrington, M. Da Costa, X. Tian, J.M. Palefsky, J.A. Doudna, CRISPR-Cas12a target binding unleashes indiscriminate single-stranded DNase activity, Science 360 (2018) 436–439. https://doi.org/10.1126/science.aar6245.
[28] S. Shmakov, O.O. Abudayyeh, K.S. Makarova, Y.I. Wolf, J.S. Gootenberg, E. Semenova, L. Minakhin, J. Joung, S. Konermann, K. Severinov, F. Zhang, E.V. Koonin, Discovery and functional characterization of diverse class 2 CRISPR-Cas systems, Mol. Cell 60 (2015) 385–397. https://doi.org/10.1016/j.molcel.2015.10.008.
[29] O.O. Abudayyeh, J.S. Gootenberg, S. Konermann, J. Joung, I.M. Slaymaker, D.B.T. Cox, S. Shmakov, K.S. Makarova, E. Semenova, L. Minakhin, K. Severinov, A. Regev, E.S. Lander, E.V. Koonin, F. Zhang, C2c2 is a single-component programmable RNA-guided RNA-targeting CRISPR effector, Science 353 (2016) aaf5573. https://doi.org/10.1126/science.aaf5573.
[30] J.S. Gootenberg, O.O. Abudayyeh, J.W. Lee, P. Essletzbichler, A.J. Dy, J. Joung, V. Verdine, N. Donghia, N.M. Daringer, C.A. Freije, C. Myhrvold, R.P. Bhattacharyya, J. Livny, A. Regev, E.V. Koonin, D.T. Hung, P.C. Sabeti, J.J. Collins, F. Zhang, Nucleic acid detection with CRISPR-Cas13a/C2c2, Science 356 (2017) 438–442. https://doi.org/10.1126/science.aam9321.
[31] A. Ramachandran, J.G. Santiago, CRISPR enzyme kinetics for molecular diagnostics, Anal. Chem. 93 (2021) 7456–7464. https://doi.org/10.1021/acs.analchem.1c00525.
[32] T. Wang, Y. Liu, H.H. Sun, B.C. Yin, B.C. Ye, An RNA-guided Cas9 nickase-based method for universal isothermal DNA amplification, Angew. Chem. 131 (2019) 5436–5440. https://doi.org/10.1002/anie.201901292.
[33] P. Fozouni, S. Son, M. Díaz de León Derby, G.J. Knott, C.N. Gray, M.V. D'Ambrosio, C. Zhao, N.A. Switz, G.R. Kumar, S.I. Stephens, D. Boehm, C.L. Tsou, J. Shu, A. Bhuiya, M. Armstrong, A.R. Harris, P.Y. Chen, J.M. Osterloh, A. Meyer-Franke, B. Joehnk, K. Walcott, A. Sil, C. Langelier, K.S. Pollard, E.D. Crawford, A.S. Puschnik, M. Phelps, A. Kistler, J.L. DeRisi, J.A. Doudna, D.A. Fletcher, M. Ott, Amplification-free detection of SARS-CoV-2 with CRISPR-Cas13a and mobile phone microscopy, Cell 184 (2021) 323–333. https://doi.org/10.1016/j.cell.2020.12.001.
[34] J.P. Broughton, X. Deng, G. Yu, C.L. Fasching, V. Servellita, J. Singh, X. Miao, J.A. Streithorst, A. Granados, A. Sotomayor-Gonzalez, K. Zorn, A. Gopez, E. Hsu, W. Gu, S. Miller, C.Y. Pan, H. Guevara, D.A. Wadford, J.S. Chen, C.Y. Chiu, CRISPR-Cas12-based detection of SARS-CoV-2, Nat. Biotechnol. 38 (2020) 870–874. https://doi.org/10.1038/s41587-020-0513-4.
[35] W. Feng, A.M. Newbigging, C. Le, B. Pang, H. Peng, Y. Cao, J. Wu, G. Abbas, J. Song, D.B. Wang, M. Cui, J. Tao, D.L. Tyrrell, X.E. Zhang, H. Zhang, X.C. Le, Molecular diagnosis of COVID-19: challenges and research needs, Anal. Chem. 92 (2020) 10196–10209. https://doi.org/10.1021/acs.analchem.0c02060.
[36] R. Nouri, Z. Tang, M. Dong, T. Liu, A. Kshirsagar, W. Guan, CRISPR-based detection of SARS-CoV-2: a review from sample to result, Biosens. Bioelectron. 178 (2021), 113012. https://doi.org/10.1016/j.bios.2021.113012.
[37] K.W. Graepel, X. Lu, J.B. Case, N.R. Sexton, E.C. Smith, M.R. Denison, Proofreading-deficient coronaviruses adapt for increased fitness over long-term passage without reversion of exoribonuclease-inactivating mutations, mBio 8 (2017), e01503. https://doi.org/10.1128/mBio.01503-17.
[38] World Health Organization (WHO), Tracking SARS-CoV-2 variants. https://www.who.int/activities/tracking-SARS-CoV-2-variants. (Accessed 17 December 2022).
[39] A. Rambaut, E.C. Holmes, Á. O'Toole, V. Hill, J.T. McCrone, C. Ruis, L. du Plessis, O.G. Pybus, A dynamic nomenclature proposal for SARS-CoV-2 lineages to assist genomic epidemiology, Nat. Microbiol. 5 (2020) 1403–1407. https://doi.org/10.1038/s41564-020-0770-5.
[40] G. Tsueng, J.L. Mullen, M. Alkuzweny, M. Cano, B. Rush, E. Haag, J. Lin, D.J. Welzel, X. Zhou, Z. Qian, A.A. Latif, E. Hufbauer, M. Zeller, K.G. Andersen, C. Wu, A.I. Su, K. Gangavarapu, L.D. Hughes, Outbreak.info Research Library: A Standardized, Searchable Platform to Discover and Explore COVID-19 Resources, bioRxiv, 2022. https://doi.org/10.1101/2022.01.20.477133.
[41] A.C. Walls, Y.J. Park, M.A. Tortorici, A. Wall, A.T. McGuire, D. Veesler, Structure, function, and antigenicity of the SARS-CoV-2 spike glycoprotein, Cell 180 (2020) 281–292. https://doi.org/10.1016/j.cell.2020.02.058.
[42] J. Lan, J. Ge, J. Yu, S. Shan, H. Zhou, S. Fan, Q. Zhang, X. Shi, Q. Wang, L. Zhang, X. Wang, Structure of the SARS-CoV-2 spike receptor-binding domain bound to the ACE2 receptor, Nature 581 (2020) 215–220. https://doi.org/10.1038/s41586-020-2180-5.
[43] M. Hoffmann, H. Kleine-Weber, S. Schroeder, N. Krüger, T. Herrler, S. Erichsen, T.S. Schiergens, G. Herrler, N.H. Wu, A. Nitsche, M.A. Müller, C. Drosten, S. Pöhlmann, SARS-CoV-2 cell entry depends on ACE2 and TMPRSS2 and is blocked by a clinically proven protease inhibitor, Cell 181 (2020) 271–280. https://doi.org/10.1016/j.cell.2020.02.052.
[44] S. Xia, Y. Zhu, M. Liu, Q. Lan, W. Xu, Y. Wu, T. Ying, S. Liu, Z. Shi, S. Jiang, L. Lu, Fusion mechanism of 2019-nCoV and fusion inhibitors targeting HR1 domain in spike protein, Cell, Mol. Immunol. 17 (2020) 765–767. https://doi.org/10.1038/s41423-020-0374-2.
[45] Protein [Internet], National Library of Medicine (US), National Center for Biotechnology Information, Bethesda (MD), 1988. – . Accession No. YP_009724390.1, surface glycoprotein [Severe acute respiratory syndrome coronavirus 2]; [cited 2022 Dec. 20]. Available from: https://www.ncbi.nlm.nih.gov/protein/YP_009724390.1.
[46] F. Krammer, SARS-CoV-2 vaccines in development, Nature 586 (2020) 516–527. https://doi.org/10.1038/s41586-020-2798-3.
[47] C.O. Barnes, C.A. Jette, M.E. Abernathy, K.A. Dam, S.R. Esswein, H.B. Gristick, A.G. Malyutin, N.G. Sharaf, K.E. Huey-Tubman, Y.E. Lee, D.F. Robbiani, M.C. Nussenzweig, A.P. West Jr., P.J. Bjorkman, SARS-CoV-2 neutralizing antibody structures inform therapeutic strategies, Nature 588 (2020) 682–687. https://doi.org/10.1038/s41586-020-2852-1.
[48] Y. Huang, C. Yang, X.F. Xu, W. Xu, S.W. Liu, Structural and functional properties of SARS-CoV-2 spike protein: potential antivirus drug development for COVID-19, Acta Pharmacol. Sin. 41 (2020) 1141–1149. https://doi.org/10.1038/s41401-020-0485-4.
[49] M.I. Barton, S.A. MacGowan, M.A. Kutuzov, O. Dushek, G.J. Barton, P.A. van der Merwe, Effects of common mutations in the SARS-CoV-2 Spike RBD and its ligand, the human ACE2 receptor on binding affinity and kinetics, Elife 10 (2021), e70658. https://doi.org/10.7554/eLife.70658.
[50] W.T. Harvey, A.M. Carabelli, B. Jackson, R.K. Gupta, E.C. Thomson, E.M. Harrison, C. Ludden, R. Reeve, A. Rambaut, COVID-19 Genomics UK (COG-UK) Consortium, S.J. Peacock, D.L. Robertson, SARS-CoV-2 variants, spike mutations and immune escape, Nat. Rev. Microbiol. 19 (2021) 409–424. https://doi.org/10.1038/s41579-021-00573-0.
[51] Protein Data Bank. https://www.rcsb.org/. (Accessed 17 December 2022).
[52] E.B. Hodcroft, CoVariants: SARS-CoV-2 Mutations and Variants of Interest, 2021. https://covariants.org/. (Accessed 17 December 2022).
[53] T.N. Starr, A.J. Greaney, S.K. Hilton, D. Ellis, K.H.D. Crawford, A.S. Dingens, M.J. Navarro, J.E. Bowen, M.A. Tortorici, A.C. Walls, N.P. King, D. Veesler, J.D. Bloom, Deep mutational scanning of SARS-CoV-2 receptor binding domain reveals constraints on folding and ACE2 binding, Cell 182 (2020) 1295–1310. https://doi.org/10.1016/j.cell.2020.08.012.
[54] F. Tian, B. Tong, L. Sun, S. Shi, B. Zheng, Z. Wang, X. Dong, P. Zheng, N501Y mutation of spike protein in SARS-CoV-2 strengthens its binding to receptor ACE2, Elife 10 (2021), e69091. https://doi.org/10.7554/eLife.69091.
[55] L. Zhang, C.B. Jackson, H. Mou, A. Ojha, H. Peng, B.D. Quinlan, E.S. Rangarajan, A. Pan, A. Vanderheiden, M.S. Suthar, W. Li, T. Izard, C. Rader, M. Farzan, H. Choe, SARS-CoV-2 spike-protein D614G mutation increases virion spike density and infectivity, Nat. Commun. 11 (2020) 6013. https://doi.org/10.1038/s41467-020-19808-4.
[56] B. Korber, W.M. Fischer, S. Gnanakaran, H. Yoon, J. Theiler, W. Abfalterer, N. Hengartner, E.E. Giorgi, T. Bhattacharya, B. Foley, K.M. Hastie, M.D. Parker, D.G. Partridge, C.M. Evans, T.M. Freeman, T.I. de Silva, C. McDanal, L.G. Perez, H. Tang, A. Moon-Walker, S.P. Whelan, C.C. LaBranche, E.O. Saphire, D.C. Montefiori, S.C.G. Grp, Tracking changes in SARS-CoV-2 spike: evidence that D614G increases infectivity of the COVID-19 virus, Cell 182 (2020) 812–827. https://doi.org/10.1016/j.cell.2020.06.043.
[57] M. McCallum, A. De Marco, F.A. Lempp, M.A. Tortorici, D. Pinto, A.C. Walls, M. Beltramello, A. Chen, Z. Liu, F. Zatta, S. Zepeda, J. di Iulio, J.E. Bowen, M. Montiel-Ruiz, J. Zhou, L.E. Rosen, S. Bianchi, B. Guarino, C.S. Fregni, R. Abdelnabi, S.Y.C. Foo, P.W. Rothlauf, L.M. Bloyet, F. Benigni, E. Cameroni, J. Neyts, A. Riva, G. Snell, A. Telenti, S.P.J. Whelan, H.W. Virgin, D. Corti, M.S. Pizzuto, D. Veesler, N-terminal domain antigenic mapping reveals a site of vulnerability for SARS-CoV-2, Cell 184 (2021) 2332–2347. https://doi.org/10.1016/j.cell.2021.03.028.
[58] P. Wang, M.S. Nair, L. Liu, S. Iketani, Y. Luo, Y. Guo, M. Wang, J. Yu, B. Zhang, P.D. Kwong, B.S. Graham, J.R. Mascola, J.Y. Chang, M.T. Yin, M. Sobieszczyk, C.A. Kyratsous, L. Shapiro, Z. Sheng, Y. Huang, D.D. Ho, Antibody resistance of SARS-CoV-2 variants B.1.351 and B.1.1.7, Nature 593 (2021) 130–135.

https://doi.org/10.1038/s41586-021-03398-2.
[59] S.A. Kemp, D.A. Collier, R.P. Datir, I.A.T.M. Ferreira, S. Gayed, A. Jahun, M. Hosmillo, C. Rees-Spear, P. Mlcochova, I.U. Lumb, D.J. Roberts, A. Chandra, N. Temperton, , The COVID-19 Genomics UK (COG-UK) Consortium, K. Sharrocks, E. Blane, Y. Modis, K.E. Leigh, J.A.G. Briggs, M.J. van Gils, K.G.C. Smith, J.R. Bradley, C. Smith, R. Doffinger, L. Ceron-Gutierrez, G. Barcenas-Morales, D.D. Pollock, R.A. Goldstein, A. Smielewska, J.P. Skittrall, T. Gouliouris, I.G. Goodfellow, E. Gkrania-Klotsas, C.J.R. Illingworth, L.E. McCoy, R.K. Gupta, SARS-CoV-2 evolution during treatment of chronic infection, Nature 592 (2021) 277–282. https://doi.org/10.1038/s41586-021-03291-y.
[60] B. Meng, S.A. Kemp, G. Papa, R. Datir, I.A.T.M. Ferreira, S. Marelli, W.T. Harvey, S. Lytras, A. Mohamed, G. Gallo, N. Thakur, D.A. Collier, P. Mlcochova, , The COVID-19 Genomics UK (COG-UK) Consortium, L.M. Duncan, A.M. Carabelli, J.C. Kenyon, A.M. Lever, A. De Marco, C. Saliba, K. Culap, E. Cameroni, N.J. Matheson, L. Piccoli, D. Corti, L.C. James, D.L. Robertson, D. Bailey, R.K. Gupta, Recurrent emergence of SARS-CoV-2 spike deletion H69/V70 and its role in the Alpha variant B.1.1.7, Cell Rep. 35 (2021), 109292. https://doi.org/10.1016/j.celrep.2021.109292.
[61] E. Volz, S. Mishra, M. Chand, J.C. Barrett, R. Johnson, L. Geidelberg, W.R. Hinsley, D.J. Laydon, G. Dabrera, Á. O'Toole, R. Amato, M. Ragonnet-Cronin, I. Harrison, B. Jackson, C.V. Ariani, O. Boyd, N.J. Loman, J.T. McCrone, S. Goncalves, D. Jorgensen, R. Myers, V. Hill, D.K. Jackson, K. Gaythorpe, N. Groves, J. Sillitoe, D.P. Kwiatkowski, , The COVID-19 Genomics UK (COG-UK) consortium, S. Flaxman, O. Ratmann, S. Bhatt, S. Hopkins, A. Gandy, A. Rambaut, N.M. Ferguson, Assessing transmissibility of SARS-CoV-2 lineage B.1.1.7 in England, Nature 593 (2021) 266–269. https://doi.org/10.1038/s41586-021-03470-x.
[62] M. Kidd, A. Richter, A. Best, N. Cumley, J. Mirza, B. Percival, M. Mayhew, O. Megram, F. Ashford, T. White, E. Moles-Garcia, L. Crawford, A. Bosworth, S.F. Atabani, T. Plant, A. McNally, S-variant SARS-CoV-2 lineage B1.1.7 is associated with significantly higher viral load in samples tested by TaqPath polymerase chain reaction, J. Infect. Dis. 223 (2021) 1666–1670. https://doi.org/10.1093/infdis/jiab082.
[63] N.G. Davies, C.I. Jarvis, W.J. Edmunds, N.P. Jewell, K. Diaz-Ordaz, R.H. Keogh, CMMID COVID-19 Working Group, Increased mortality in community-tested cases of SARS-CoV-2 lineage B.1.1.7, Nature 593 (2021) 270–274. https://doi.org/10.1038/s41586-021-03426-1.
[64] H. Tegally, E. Wilkinson, M. Giovanetti, A. Iranzadeh, V. Fonseca, J. Giandhari, D. Doolabh, S. Pillay, E.J. San, N. Msomi, K. Mlisana, A. von Gottberg, S. Walaza, M. Allam, A. Ismail, T. Mohale, A.J. Glass, S. Engelbrecht, G. Van Zyl, W. Preiser, F. Petruccione, A. Sigal, D. Hardie, G. Marais, N.Y. Hsiao, S. Korsman, M.A. Davies, L. Tyers, I. Mudau, D. York, C. Maslo, D. Goedhals, S. Abrahams, O. Laguda-Akingba, A. Alisoltani-Dehkordi, A. Godzik, C.K. Wibmer, B.T. Sewell, J. Lourenco, L.C.J. Alcantara, S.L. Kosakovsky Pond, S. Weaver, D. Martin, R.J. Lessells, J.N. Bhiman, C. Williamson, T. de Oliveira, Detection of a SARS-CoV-2 variant of concern in South Africa, Nature 592 (2021) 438–443. https://doi.org/10.1038/s41586-021-03402-9.
[65] D. Zhou, W. Dejnirattisai, P. Supasa, C. Liu, A.J. Mentzer, H.M. Ginn, Y. Zhao, H.M.E. Duyvesteyn, A. Tuekprakhon, R. Nutalai, B. Wang, G.C. Paesen, C. Lopez-Camacho, J. Slon-Campos, B. Hallis, N. Coombes, K. Bewley, S. Charlton, T.S. Walter, D. Skelly, S.F. Lumley, C. Dold, R. Levin, T. Dong, A.J. Pollard, J.C. Knight, D. Crook, T. Lambe, E. Clutterbuck, S. Bibi, A. Flaxman, M. Bittaye, S. Belij-Rammerstorfer, S. Gilbert, W. James, M.W. Carroll, P. Klenerman, E. Barnes, S.J. Dunachie, E.E. Fry, J. Mongkolsapaya, J. Ren, D.I. Stuart, G.R. Screaton, Evidence of escape of SARS-CoV-2 variant B.1.351 from natural and vaccine-induced sera, Cell 189 (2021) 2348–2361. https://doi.org/10.1016/j.cell.2021.02.037.
[66] S. Jangra, C. Ye, R. Rathnasinghe, D. Stadlbauer, F. Krammer, V. Simon, L. Martinez-Sobrido, A. Garcia-Sastre, M. Schotsaert, Personalized Virology Initiative study group, SARS-CoV-2 spike E484K mutation reduces antibody neutralisation, Lancet Microbe 2 (2021), e283–e284. https://doi.org/10.1016/S2666-5247(21)00068-9.
[67] H. Tegally, E. Wilkinson, R.J. Lessells, J. Giandhari, S. Pillay, N. Msomi, K. Mlisana, J.N. Bhiman, A. von Gottberg, S. Walaza, V. Fonseca, M. Allam, A. Ismail, A.J. Glass, S. Engelbrecht, G. Van Zyl, W. Preiser, C. Williamson, F. Petruccione, A. Sigal, I. Gazy, D. Hardie, N.Y. Hsiao, D. Martin, D. York, D. Goedhals, E.J. San, M. Giovanetti, J. Lourenco, L.C.J. Alcantara, T. de Oliveira, Sixteen novel lineages of SARS-CoV-2 in South Africa, Nat. Med. 27 (2021) 440–446. https://doi.org/10.1038/s41591-021-01255-3.
[68] M. Hoffmann, P. Arora, R. Groß, A. Seidel, B.F. Hörnich, A.S. Hahn, N. Krüger, L. Graichen, H. Hofmann-Winkler, A. Kempf, M.S. Winkler, S. Schulz, H.M. Jäck, B. Jahrsdörfer, H. Schrezenmeier, M. Müller, A. Kleger, J. Münch, S. Pöhlmann, SARS-CoV-2 variants B.1.351 and P.1 escape from neutralizing antibodies, Cell 184 (2021) 2384–2393. https://doi.org/10.1016/j.cell.2021.03.036.
[69] N.R. Faria, T.A. Mellan, C. Whittaker, I.M. Claro, D.D.S. Candido, S. Mishra, M.A.E. Crispim, F.C. Sales, I. Hawryluk, J.T. McCrone, R.J.G. Hulswit, L.A.M. Franco, M.S. Ramundo, J.G. de Jesus, P.S. Andrade, T.M. Coletti, G.M. Ferreira, C.A.M. Silva, E.R. Manuli, R.H.M. Pereira, P.S. Peixoto, M.U.G. Kraemer, N. Gaburo Jr., C.D.C. Camilo, H. Hoeltgebaum, W.M. Souza, E.C. Rocha, L.M. de Souza, M.C. de Pinho, L.J.T. Araujo, F.S.V. Malta, A.B. de Lima, J.D. Silva, D.A.G. Zauli, A.C.D. Ferreira, R.P. Schnekenberg, D.J. Laydon, P.G.T. Walker, H.M. Schlüter, A.L.P. dos Santos, M.S. Vidal, V.S. Del Caro, R.M.F. Filho, H.M. dos Santos, R.S. Aguiar, J.L.P. Proenca-Modena, B. Nelson, J.A. Hay, M. Monod, X. Miscouridou, H. Coupland, R. Sonabend, M. Vollmer, A. Gandy, C.A. Prete Jr., V.H. Nascimento, M.A. Suchard, T.A. Bowden, S.L.K. Pond, C.H. Wu, O. Ratmann, N.M. Ferguson, C. Dye, N.J. Loman, P. Lemey, A. Rambaut, N.A. Fraiji, M.D.S.S. Carvalho, O.G. Pybus, S. Flaxman, S. Bhatt, E.C. Sabino, Genomics and epidemiology of the P.1 SARS-CoV-2 lineage in Manaus, Brazil, Science 372 (2021) 815–821. https://doi.org/10.1126/science.abh2644.
[70] A.R.R. Freitas, O.A. Beckedorff, L.P. de Góes Cavalcanti, A.M. Siqueira, D.B. de Castro, C.F. da Costa, D.R.Q. Lemos, E.N. Barros, The emergence of novel SARS-CoV-2 variant P.1 in Amazonas (Brazil) was temporally associated with a change in the age and sex profile of COVID-19 mortality: a population based ecological study, The Lancet Regional Health-Americas 1 (2021), 100021. https://doi.org/10.1016/j.lana.2021.100021.
[71] S. Cherian, V. Potdar, S. Jadhav, P. Yadav, N. Gupta, M. Das, P. Rakshit, S. Singh, P. Abraham, S. Panda, NIC Team, SARS-CoV-2 spike mutations, L452R, T478K, E484Q and P681R in the second wave of COVID-19 in Maharashtra, India, Microorganisms 9 (2021) 1542. https://doi.org/10.3390/microorganisms9071542.
[72] Q. Li, J. Wu, J. Nie, L. Zhang, H. Hao, S. Liu, C. Zhao, Q. Zhang, H. Liu, L. Nie, H. Qin, M. Wang, Q. Lu, X. Li, Q. Sun, J. Liu, L. Zhang, X. Li, W. Huang, Y. Wang, The impact of mutations in SARS-CoV-2 spike on viral infectivity and antigenicity, Cell 182 (2020) 1284–1294. https://doi.org/10.1016/j.cell.2020.07.012.
[73] P. Mlcochova, S.A. Kemp, M.S. Dhar, G. Papa, B. Meng, I. Ferreira, R. Datir, D.A. Collier, A. Albecka, S. Singh, R. Pandey, J. Brown, J. Zhou, N. Goonawardane, S. Mishra, C. Whittaker, T. Mellan, R. Marwal, M. Datta, S. Sengupta, K. Ponnusamy, V.S. Radhakrishnan, A. Abdullahi, O. Charles, P. Chattopadhyay, P. Devi, D. Caputo, T. Peacock, C. Wattal, N. Goel, A. Satwik, R. Vaishya, M. Agarwal, S.-C.-G.C. Indian, C. Genotype to Phenotype Japan, C.-N.B.C.- Collaboration, A. Mavousian, J.H. Lee, J. Bassi, C. Silacci-Fegni, C. Saliba, D. Pinto, T. Irie, I. Yoshida, W.L. Hamilton, K. Sato, S. Bhatt, S. Flaxman, L.C. James, D. Corti, L. Piccoli, W.S. Barclay, P. Rakshit, A. Agrawal, R.K. Gupta, SARS-CoV-2 B.1.617.2 Delta variant replication and immune evasion, Nature 599 (2021) 114–119. https://doi.org/10.1038/s41586-021-03944-y.
[74] B. Li, A. Deng, K. Li, Y. Hu, Z. Li, Y. Shi, Q. Xiong, Z. Liu, Q. Guo, L. Zou, H. Zhang, M. Zhang, F. Ouyang, J. Su, W. Su, J. Xu, H. Lin, J. Sun, J. Peng, H. Jiang, P. Zhou, T. Hu, M. Luo, Y. Zhang, H. Zheng, J. Xiao, T. Liu, M. Tan, R. Che, H. Zeng, Z. Zheng, Y. Huang, J. Yu, L. Yi, J. Wu, J. Chen, H. Zhong, X. Deng, M. Kang, O.G. Pybus, M. Hall, K.A. Lythgoe, Y. Li, J. Yuan, J. He, J. Lu, Viral infection and transmission in a large, well-traced outbreak caused by the SARS-CoV-2 Delta variant, Nat. Commun. 13 (2022) 460. https://doi.org/10.1038/s41467-022-28089-y.
[75] S. Shiehzadegan, N. Alaghemand, M. Fox, V. Venketaraman, Analysis of the delta variant B.1.617.2 COVID-19, Clin. Pract. 11 (2021) 778–784. https://doi.org/10.3390/clinpract11040093.
[76] P.A. Christensen, R.J. Olsen, S.W. Long, S. Subedi, J.J. Davis, P. Hodjat, D.R. Walley, J.C. Kinskey, M.O. Saavedra, L. Pruitt, K. Reppond, M.N. Shyer, J. Cambric, R. Gadd, R.M. Thakur, A. Batajoo, R. Mangham, S. Pena, T. Trinh, P. Yerramilli, M. Nguyen, R. Olson, R. Snehal, J. Gollihar, J.M. Musser, Delta variants of SARS-CoV-2 cause significantly increased vaccine breakthrough COVID-19 cases in Houston, Texas, Am. J. Pathol. 192 (2022) 320–331. https://doi.org/10.1016/j.ajpath.2021.10.019.
[77] K.A. Twohig, T. Nyberg, A. Zaidi, S. Thelwall, M.A. Sinnathamby, S. Aliabadi, S.R. Seaman, R.J. Harris, R. Hope, J. Lopez-Bernal, E. Gallagher, A. Charlett, D. De Angelis, A.M. Presanis, G. Dabrera, COVID-19 Genomics UK (COG-UK) consortium, Hospital admission and emergency care attendance risk for SARS-CoV-2 delta (B.1.617.2) compared with alpha (B.1.1.7) variants of concern: a cohort study, Lancet Infect. Dis. 22 (2022) 35–42. https://doi.org/10.1016/S1473-3099(21)00475-8.
[78] W. Dejnirattisai, J. Huo, D. Zhou, J. Zahradnik, P. Supasa, C. Liu, H.M.E. Duyvesteyn, H.M. Ginn, A.J. Mentzer, A. Tuekprakhon, R. Nutalai, B. Wang, A. Dijokaite, S. Khan, O. Avinoam, M. Bahar, D. Skelly, S. Adele, S.A. Johnson, A. Amini, T.G. Ritter, C. Mason, C. Dold, D. Pan, S. Assadi, A. Bellass, N. Omo-Dare, D. Koeckerling, A. Flaxman, D. Jenkin, P.K. Aley, M. Voysey, S.A. Costa Clemens, F.G. Naveca, V. Nascimento, F. Nascimento, C. Fernandes da Costa, P.C. Resende, A. Pauvolid-Correa, M.M. Siqueira, V. Baillie, N. Serafin, G. Kwatra, K. Da Silva, S.A. Madhi, M.C. Nunes, T. Malik, P.J.M. Openshaw, J.K. Baillie, M.G. Semple, A.R. Townsend, K.A. Huang, T.K. Tan, M.W. Carroll, P. Klenerman, E. Barnes, S.J. Dunachie, B. Constantinides, H. Webster, D. Crook, A.J. Pollard, T. Lambe, O. Consortium, I.C. Consortium, N.G. Paterson, M.A. Williams, D.R. Hall, E.E. Fry, J. Mongkolsapaya, J. Ren, G. Schreiber, D.I. Stuart, G.R. Screaton, SARS-CoV-2 Omicron-B.1.1.529 leads to widespread escape from neutralizing antibody responses, Cell 185 (2022) 467–484. https://doi.org/10.1016/j.cell.2021.12.046.
[79] J.Y. Yu, A.Y. Collier, M. Rowe, F. Mardas, J.D. Ventura, H. Wan, J. Miller, O. Powers, B. Chung, M. Siamatu, N.P. Hachmann, N. Surve, F. Nampanya, A. Chandrashekar, D.H. Barouch, Neutralization of the SARS-CoV-2 omicron BA.1 and BA.2 variants, N. Engl. J. Med. 386 (2022) 1579–1580. https://doi.org/10.1056/NEJMc2201849.
[80] H.H. Webster, T. Nyberg, M.A. Sinnathamby, N.A. Aziz, N. Ferguson, G. Seghezzo, P.B. Blomquist, J. Bridgen, M. Chand, N. Groves, R. Myers, R. Hope, E. Ashano, J. Lopez-Bernal, D. De Angelis, G. Dabrera, A.M. Presanis, S. Thelwall, Hospitalisation and mortality risk of SARS-COV-2 variant omicron sub-lineage BA.2 compared to BA.1 in England, Nat. Commun. 13 (2022)

6053. https://doi.org/10.1038/s41467-022-33740-9.
[81] E. Mahase, Omicron sub-lineage BA. 2 may have "substantial growth advantage," UKHSA reports, BMJ 376 (2022) o263. https://doi.org/10.1136/bmj.o263.
[82] A. Tuekprakhon, R. Nutalai, A. Dijokaite-Guraliuc, D. Zhou, H.M. Ginn, M. Selvaraj, C. Liu, A.J. Mentzer, P. Supasa, H.M.E. Duyvesteyn, R. Das, D. Skelly, T.G. Ritter, A. Amini, S. Bibi, S. Adele, S.A. Johnson, B. Constantinides, H. Webster, N. Temperton, P. Klenerman, E. Barnes, S.J. Dunachie, D. Crook, A.J. Pollard, T. Lambe, P. Goulder, N.G. Paterson, M.A. Williams, D.R. Hall, O. Consortium, I.C. Consortium, E.E. Fry, J. Huo, J. Mongkolsapaya, J. Ren, D.I. Stuart, G.R. Screaton, Antibody escape of SARS-CoV-2 Omicron BA.4 and BA.5 from vaccine and BA.1 serum, Cell 185 (2022) 2422–2433. https://doi.org/10.1016/j.cell.2022.06.005.
[83] H. Tegally, M. Moir, J. Everatt, M. Giovanetti, C. Scheepers, E. Wilkinson, K. Subramoney, Z. Makatini, S. Moyo, D.G. Amoako, C. Baxter, C.L. Althaus, U.J. Anyaneji, D. Kekana, R. Viana, J. Giandhari, R.J. Lessells, T. Maponga, D. Maruapula, W. Choga, M. Matshaba, M.B. Mbulawa, N. Msomi, N.S. consortium, Y. Naidoo, S. Pillay, T.J. Sanko, J.E. San, L. Scott, L. Singh, N.A. Magini, P. Smith-Lawrence, W. Stevens, G. Dor, D. Tshiabuila, N. Wolter, W. Preiser, F.K. Treurnicht, M. Venter, G. Chiloane, C. McIntyre, A. O'Toole, C. Ruis, T.P. Peacock, C. Roemer, S.L. Kosakovsky Pond, C. Williamson, O.G. Pybus, J.N. Bhiman, A. Glass, D.P. Martin, B. Jackson, A. Rambaut, O. Laguda-Akingba, S. Gaseitsiwe, A. von Gottberg, T. de Oliveira, Emergence of SARS-CoV-2 omicron lineages BA.4 and BA.5 in South Africa, Nat. Med. 28 (2022) 1785–1790. https://doi.org/10.1038/s41591-022-01911-2.
[84] M. Shah, H.G. Woo, Omicron: a heavily mutated SARS-CoV-2 variant exhibits stronger binding to ACE2 and potently escapes approved COVID-19 therapeutic antibodies, Front. Immunol. 12 (2021), 830527. https://doi.org/10.3389/fimmu.2021.830527.
[85] R. Viana, S. Moyo, D.G. Amoako, H. Tegally, C. Scheepers, C.L. Althaus, U.J. Anyaneji, P.A. Bester, M.F. Boni, M. Chand, W.T. Choga, R. Colquhoun, M. Davids, K. Deforche, D. Doolabh, L. du Plessis, S. Engelbrecht, J. Everatt, J. Giandhari, M. Giovanetti, D. Hardie, V. Hill, N.Y. Hsiao, A. Iranzadeh, A. Ismail, C. Joseph, R. Joseph, L. Koopile, S.L. Kosakovsky Pond, M.U.G. Kraemer, L. Kuate-Lere, O. Laguda-Akingba, O. Lesetedi-Mafoko, R.J. Lessells, S. Lockman, A.G. Lucaci, A. Maharaj, B. Mahlangu, T. Maponga, K. Mahlakwane, Z. Makatini, G. Marais, D. Maruapula, K. Masupu, M. Matshaba, S. Mayaphi, N. Mbhele, M.B. Mbulawa, A. Mendes, K. Mlisana, A. Mnguni, T. Mohale, M. Moir, K. Moruisi, M. Mosepele, G. Motsatsi, M.S. Motswaledi, T. Mphoyakgosi, N. Msomi, P.N. Mwangi, Y. Naidoo, N. Ntuli, M. Nyaga, L. Olubayo, S. Pillay, B. Radibe, Y. Ramphal, U. Ramphal, J.E. San, L. Scott, R. Shapiro, L. Singh, P. Smith-Lawrence, W. Stevens, A. Strydom, K. Subramoney, N. Tebeila, D. Tshiabuila, J. Tsui, S. van Wyk, S. Weaver, C.K. Wibmer, E. Wilkinson, N. Wolter, A.E. Zarebski, B. Zuze, D. Goedhals, W. Preiser, F. Treurnicht, M. Venter, C. Williamson, O.G. Pybus, J. Bhiman, A. Glass, D.P. Martin, A. Rambaut, S. Gaseitsiwe, A. von Gottberg, T. de Oliveira, Rapid epidemic expansion of the SARS-CoV-2 Omicron variant in southern Africa, Nature 603 (2022) 679–686. https://doi.org/10.1038/s41586-022-04411-y.
[86] D. Tian, Y. Sun, H. Xu, Q. Ye, The emergence and epidemic characteristics of the highly mutated SARS-CoV-2 Omicron variant, J. Med. Virol. 94 (2022) 2376–2383. https://doi.org/10.1002/jmv.27643.
[87] A.M. Syed, A. Ciling, T.Y. Taha, I.P. Chen, M.M. Khalid, B. Sreekumar, P.Y. Chen, G.R. Kumar, R. Suryawanshi, I. Silva, B. Milbes, N. Kojima, V. Hess, M. Shacreaw, L. Lopez, M. Brobeck, F. Turner, L. Spraggon, T. Tabata, M. Ott, J.A. Doudna, Omicron mutations enhance infectivity and reduce antibody neutralization of SARS-CoV-2 virus-like particles, Proc. Natl. Acad. Sci. U.S.A. 119 (2022), e2200592119. https://doi.org/10.1073/pnas.2200592119.
[88] C. Kurhade, J. Zou, H.J. Xia, H. Cai, Q. Yang, M. Cutler, D. Cooper, A. Muik, K.U. Jansen, X. Xie, K.A. Swanson, P.Y. Shi, Neutralization of Omicron BA.1, BA.2, and BA.3 SARS-CoV-2 by 3 doses of BNT162b2 vaccine, Nat. Commun. 13 (2022) 3602. https://doi.org/10.1038/s41467-022-30681-1.
[89] P.A. Christensen, R.J. Olsen, S.W. Long, R. Snehal, J.J. Davis, M.O. Saavedra, K. Reppond, M.N. Shyer, J. Cambric, R. Gadd, R.M. Thakur, A. Batajoo, R. Mangham, S. Pena, T. Trinh, J.C. Kinskey, G. Williams, R. Olson, J. Gollihar, J.M. Musser, Signals of significantly increased vaccine breakthrough, decreased hospitalization rates, and less severe disease in patients with coronavirus disease 2019 caused by the Omicron variant of severe acute respiratory syndrome coronavirus 2 in Houston, Texas, Am. J. Pathol. 192 (2022) 642–652. https://doi.org/10.1016/j.ajpath.2022.01.007.
[90] Y. Cao, A. Yisimayi, F. Jian, W. Song, T. Xiao, L. Wang, S. Du, J. Wang, Q. Li, X. Chen, Y. Yu, P. Wang, Z. Zhang, P. Liu, R. An, X. Hao, Y. Wang, J. Wang, R. Feng, H. Sun, L. Zhao, W. Zhang, D. Zhao, J. Zheng, L. Yu, C. Li, N. Zhang, R. Wang, X. Niu, S. Yang, X. Song, Y. Chai, Y. Hu, Y. Shi, L. Zheng, Z. Li, Q. Gu, F. Shao, W. Huang, R. Jin, Z. Shen, Y. Wang, X. Wang, J. Xiao, X.S. Xie, BA.2.12.1, BA.4 and BA.5 escape antibodies elicited by Omicron infection, Nature 608 (2022) 593–602. https://doi.org/10.1038/s41586-022-04980-y.
[91] I. Kimura, D. Yamasoba, T. Tamura, N. Nao, T. Suzuki, Y. Oda, S. Mitoma, J. Ito, H. Nasser, J. Zahradnik, K. Uriu, S. Fujita, Y. Kosugi, L. Wang, M. Tsuda, M. Kishimoto, H. Ito, R. Suzuki, R. Shimizu, M.M. Begum, K. Yoshimatsu, K.T. Kimura, J. Sasaki, K. Sasaki-Tabata, Y. Yamamoto, T. Nagamoto, J. Kanamune, K. Kobiyama, H. Asakura, M. Nagashima, K. Sadamasu, K. Yoshimura, K. Shirakawa, A. Takaori-Kondo, J. Kuramochi, G. Schreiber, K.J. Ishii, C. Genotype to Phenotype Japan, T. Hashiguchi, T. Ikeda, A. Saito, T. Fukuhara, S. Tanaka, K. Matsuno, K. Sato, Virological characteristics of the SARS-CoV-2 Omicron BA.2 subvariants, including BA.4 and BA.5, Cell 185 (2022) 3992–4007. https://doi.org/10.1016/j.cell.2022.09.018.
[92] N. Wolter, W. Jassat, S. Walaza, R. Welch, H. Moultrie, M.J. Groome, D.G. Amoako, J. Everatt, J.N. Bhiman, C. Scheepers, N. Tebeila, N. Chiwandire, M. du Plessis, N. Govender, A. Ismail, A. Glass, K. Mlisana, W. Stevens, F.K. Treurnicht, K. Subramoney, Z. Makatini, N.Y. Hsiao, R. Parboosing, J. Wadula, H. Hussey, M.A. Davies, A. Boulle, A. von Gottberg, C. Cohen, Clinical severity of SARS-CoV-2 Omicron BA.4 and BA.5 lineages compared to BA.1 and Delta in South Africa, Nat. Commun. 13 (2022) 5860. https://doi.org/10.1038/s41467-022-33614-0.
[93] S.P. Chaki, M.M. Kahl-McDonagh, B.W. Neuman, K.A. Zuelke, Receptor-binding-motif-targeted Sanger sequencing: a quick and cost-effective strategy for molecular surveillance of SARS-CoV-2 variants, Microbiol. Spectr. 10 (2022), e0066522. https://doi.org/10.1128/spectrum.00665-22.
[94] A. Chappleboim, D. Joseph-Strauss, A. Rahat, I. Sharkia, M. Adam, D. Kitsberg, G. Fialkoff, M. Lotem, O. Gershon, A.K. Schmidtner, E. Oiknine-Djian, A. Klochendler, R. Sadeh, Y. Dor, D. Wolf, N. Habib, N. Friedman, Early sample tagging and pooling enables simultaneous SARS-CoV-2 detection and variant sequencing, Sci. Transl. Med. 13 (2021), eabj2266. https://doi.org/10.1126/scitranslmed.abj2266.
[95] A. Yermanos, K.-L. Hong, A. Agrafiotis, J. Han, S. Nadeau, C. Valenzuela, A. Azizoglu, R. Ehling, B. Gao, M. Spahr, DeepSARS: simultaneous diagnostic detection and genomic surveillance of SARS-CoV-2, BMC Genom. 23 (2022), 289. https://doi.org/10.1186/s12864-022-08403-0.
[96] A. Nasereddin, H. Golan Berman, D.G. Wolf, E. Oiknine-Djian, S. Adar, Identification of SARS-CoV-2 variants of concern using amplicon next-generation sequencing, Microbiol. Spectr. 10 (2022), e0073622. https://doi.org/10.1128/spectrum.00736-22.
[97] G.E. Wagner, M.G. Totaro, A. Volland, M. Lipp, S. Saiger, S. Lichtenegger, P. Forstner, D. von Laer, G. Oberdorfer, I. Steinmetz, A Novel High-throughput nanopore-sequencing-based strategy for rapid and automated S-Protein typing of SARS-CoV-2 variants, Viruses 13 (2021) 2548. https://doi.org/10.3390/v13122548.
[98] P.S. Yeung, H. Wang, M. Sibai, D. Solis, F. Yamamoto, N. Iwai, B. Jiang, N. Hammond, B. Truong, S. Bihon, S. Santos, M. Mar, C. Mai, K.O. Mfuh, J.A. Miller, C. Huang, M.K. Sahoo, J.L. Zehnder, B.A. Pinsky, Evaluation of a rapid and accessible reverse transcription-quantitative PCR approach for SARS-CoV-2 variant of concern identification, J. Clin. Microbiol. 60 (2022), e00178-22. https://doi.org/10.1128/jcm.00178-22.
[99] J.A. Garson, S. Badru, E. Parker, R.S. Tedder, M.O. McClure, Highly sensitive and specific detection of the SARS-CoV-2 Delta variant by double-mismatch allele-specific real time reverse transcription PCR, J. Clin. Virol. 146 (2022), 105049. https://doi.org/10.1016/j.jcv.2021.105049.
[100] O. Erster, E. Mendelson, A. Kabat, V. Levy, B. Mannasse, H. Assraf, R. Azar, Y. Ali, E. Bucris, D. Bar-Ilan, O. Mor, M. Elul, M. Mandelboim, D. Sofer, S. Fleishon, N.S. Zuckerman, I. Bar-Or, Specific detection of SARS-CoV-2 variants B.1.1.7 (Alpha) and B.1.617.2 (Delta) using a one-step quantitative PCR assay, Microbiol. Spectr. 10 (2022), e02176-21. https://doi.org/10.1128/spectrum.02176-21.
[101] Y. Wang, Y. Zhang, J. Chen, M. Wang, T. Zhang, W. Luo, Y. Li, Y. Wu, B. Zeng, K. Zhang, R. Deng, W. Li, Detection of SARS-CoV-2 and its mutated variants via CRISPR-Cas13-based transcription amplification, Anal. Chem. 93 (2021) 3393–3402. https://doi.org/10.1021/acs.analchem.0c04303.
[102] T. Zhang, W. Zhao, W. Zhao, Y. Si, N. Chen, X. Chen, X. Zhang, L. Fan, G. Sui, Universally stable and precise CRISPR-LAMP detection platform for precise multiple respiratory tract virus diagnosis including mutant SARS-CoV-2 spike N501Y, Anal. Chem. 93 (2021) 16184–16193. https://doi.org/10.1021/acs.analchem.1c04065.
[103] M. Kumar, S. Gulati, A.H. Ansari, R. Phutela, S. Acharya, M. Azhar, J. Murthy, P. Kathpalia, A. Kanakan, R. Maurya, J.S. Vasudevan, A.S. R. Pandey, S. Maiti, D. Chakraborty, FnCas9-based CRISPR diagnostic for rapid and accurate detection of major SARS-CoV-2 variants on a paper strip, Elife 10 (2021), e67130. https://doi.org/10.7554/eLife.67130.
[104] X. Huang, F. Zhang, K. Zhu, W. Lin, W. Ma, dsmCRISPR: dual synthetic mismatches CRISPR/Cas12a-based detection of SARS-CoV-2 D614G mutation, Virus Res. 304 (2021), 198530. https://doi.org/10.1016/j.virusres.2021.198530.
[105] Q. Meng, X. Wang, Y. Wang, L. Dang, X. Liu, X. Ma, T. Chi, X. Wang, Q. Zhao, G. Yang, M. Liu, X. Huang, P. Ma, Detection of the SARS-CoV-2 D614G mutation using engineered Cas12a guide RNA, Biotechnol. J. 16 (2021), e2100040. https://doi.org/10.1002/biot.202100040.
[106] J. Yang, N. Barua, M.N. Rahman, N. Lo, T.F. Tsang, X. Yang, P.K.S. Chan, L. Zhang, M. Ip, Chimeric crRNA improves CRISPR-Cas12a specificity in the N501Y mutation detection of Alpha, Beta, Gamma, and Mu variants of SARS-CoV-2, PLoS One 16 (2021), e0261778. https://doi.org/10.1371/journal.pone.0261778.
[107] B. Ning, B.M. Youngquist, D.D. Li, C.J. Lyon, A. Zelazny, N.J. Maness, D. Tian, T.Y. Hu, Rapid detection of multiple SARS-CoV-2 variants of concern by PAM-targeting mutations, Cell Rep. Methods 2 (2022), 100173. https://doi.org/10.1016/j.crmeth.2022.100173.
[108] J. Arizti-Sanz, A. Bradley, Y.B. Zhang, C.K. Boehm, C.A. Freije, M.E. Grunberg, T.F. Kosoko-Thoroddsen, N.L. Welch, P.P. Pillai, S. Mantena, G. Kim, J.N. Uwanibe, O.G. John, P.E. Eromon, G. Kocher, R. Gross, J.S. Lee, L.E. Hensley, B.L. MacInnis, J. Johnson, M. Springer, C.T. Happi, P.C. Sabeti, C. Myhrvold, Simplified Cas13-based assays for the fast identification of SARS-CoV-2 and

its variants, Nat. Biomed. Eng. 6 (2022) 932–943. https://doi.org/10.1038/s41551-022-00889-z.
[109] W. Zhou, L. Hu, L. Ying, Z. Zhao, P.K. Chu, X.F. Yu, A CRISPR-Cas9-triggered strand displacement amplification method for ultrasensitive DNA detection, Nat. Commun. 9 (2018) 5012. https://doi.org/10.1038/s41467-018-07324-5.
[110] F. Jiang, D.W. Taylor, J.S. Chen, J.E. Kornfeld, K. Zhou, A.J. Thompson, E. Nogales, J.A. Doudna, Structures of a CRISPR-Cas9 R-loop complex primed for DNA cleavage, Science 351 (2016) 867–871. https://doi.org/10.1126/science.aad8282.
[111] G. Gasiunas, R. Barrangou, P. Horvath, V. Siksnys, Cas9-crRNA ribonucleoprotein complex mediates specific DNA cleavage for adaptive immunity in bacteria, Proc. Natl. Acad. Sci. U.S.A. 109 (2012) E2579–E2586. https://doi.org/10.1073/pnas.1208507109.
[112] F.A. Ran, P.D. Hsu, C.Y. Lin, J.S. Gootenberg, S. Konermann, A.E. Trevino, D.A. Scott, A. Inoue, S. Matoba, Y. Zhang, F. Zhang, Double nicking by RNA-guided CRISPR Cas9 for enhanced genome editing specificity, Cell 154 (2013) 1380–1389. https://doi.org/10.1016/j.cell.2013.08.021.
[113] L.S. Qi, M.H. Larson, L.A. Gilbert, J.A. Doudna, J.S. Weissman, A.P. Arkin, W.A. Lim, Repurposing CRISPR as an RNA-guided platform for sequence-specific control of gene expression, Cell 152 (2013) 1173–1183. https://doi.org/10.1016/j.cell.2013.02.022.
[114] X. Wu, D.A. Scott, A.J. Kriz, A.C. Chiu, P.D. Hsu, D.B. Dadon, A.W. Cheng, A.E. Trevino, S. Konermann, S. Chen, R. Jaenisch, F. Zhang, P.A. Sharp, Genome-wide binding of the CRISPR endonuclease Cas9 in mammalian cells, Nat. Biotechnol. 32 (2014) 670–676. https://doi.org/10.1038/nbt.2889.
[115] V. Pattanayak, S. Lin, J.P. Guilinger, E. Ma, J.A. Doudna, D.R. Liu, High-throughput profiling of off-target DNA cleavage reveals RNA-programmed Cas9 nuclease specificity, Nat. Biotechnol. 31 (2013) 839–843. https://doi.org/10.1038/nbt.2673.
[116] P.D. Hsu, D.A. Scott, J.A. Weinstein, F.A. Ran, S. Konermann, V. Agarwala, Y. Li, E.J. Fine, X. Wu, O. Shalem, T.J. Cradick, L.A. Marraffini, G. Bao, F. Zhang, DNA targeting specificity of RNA-guided Cas9 nucleases, Nat. Biotechnol. 31 (2013) 827–832. https://doi.org/10.1038/nbt.2647.
[117] Y. Fu, J.D. Sander, D. Reyon, V.M. Cascio, J.K. Joung, Improving CRISPR-Cas nuclease specificity using truncated guide RNAs, Nat. Biotechnol. 32 (2014) 279–284. https://doi.org/10.1038/nbt.2808.
[118] Y.S. Dagdas, J.S. Chen, S.H. Sternberg, J.A. Doudna, A. Yildiz, A conformational checkpoint between DNA binding and cleavage by CRISPR-Cas9, Sci. Adv. 3 (2017), eaao0027. https://doi.org/10.1126/sciadv.aao0027.
[119] S.W. Cho, S. Kim, Y. Kim, J. Kweon, H.S. Kim, S. Bae, J.S. Kim, Analysis of off-target effects of CRISPR/Cas-derived RNA-guided endonucleases and nickases, Genome Res. 24 (2014) 132–141. https://doi.org/10.1101/gr.162339.113.
[120] C.R. Cromwell, K. Sung, J. Park, A.R. Krysler, J. Jovel, S.K. Kim, B.P. Hubbard, Incorporation of bridged nucleic acids into CRISPR RNAs improves Cas9 endonuclease specificity, Nat. Commun. 9 (2018) 1448. https://doi.org/10.1038/s41467-018-03927-0.
[121] M. Rahdar, M.A. McMahon, T.P. Prakash, E.E. Swayze, C.F. Bennett, D.W. Cleveland, Synthetic CRISPR RNA-Cas9-guided genome editing in human cells, Proc. Natl. Acad. Sci. U.S.A. 112 (2015) E7110–E7117. https://doi.org/10.1073/pnas.1520883112.
[122] D.D. Kocak, E.A. Josephs, V. Bhandarkar, S.S. Adkar, J.B. Kwon, C.A. Gersbach, Increasing the specificity of CRISPR systems with engineered RNA secondary structures, Nat. Biotechnol. 37 (2019) 657–666. https://doi.org/10.1038/s41587-019-0095-1.
[123] J. Song, B. Cha, J. Moon, H. Jang, S. Kim, J. Jang, D. Yong, H.J. Kwon, I.C. Lee, E.K. Lim, J. Jung, H.G. Park, T. Kang, Smartphone-based SARS-CoV-2 and variants detection system using colorimetric DNAzyme reaction triggered by loop-mediated isothermal amplification (LAMP) with clustered regularly interspaced short palindromic repeats (CRISPR), ACS Nano 16 (2022) 11300–11314. https://doi.org/10.1021/acsnano.2c04840.
[124] L.B. Harrington, D. Burstein, J.S. Chen, D. Paez-Espino, E. Ma, I.P. Witte, J.C. Cofsky, N.C. Kyrpides, J.F. Banfield, J.A. Doudna, Programmed DNA destruction by miniature CRISPR-Cas14 enzymes, Science 362 (2018) 839–842. https://doi.org/10.1126/science.aav4294.
[125] D.C. Swarts, M. Jinek, Mechanistic insights into the *cis*- and *trans*-acting DNase activities of Cas12a, Mol. Cell 73 (2019) 589–600. https://doi.org/10.1016/j.molcel.2018.11.021.
[126] T. Yamano, H. Nishimasu, B. Zetsche, H. Hirano, I.M. Slaymaker, Y. Li, I. Fedorova, T. Nakane, K.S. Makarova, E.V. Koonin, R. Ishitani, F. Zhang, O. Nureki, Crystal structure of Cpf1 in complex with guide RNA and target DNA, Cell 165 (2016) 949–962. https://doi.org/10.1016/j.cell.2016.04.003.
[127] S. Stella, P. Alcón, G. Montoya, Structure of the Cpf1 endonuclease R-loop complex after target DNA cleavage, Nature 546 (2017) 559–563. https://doi.org/10.1038/nature22398.
[128] E.A. Nalefski, N. Patel, P.J.Y. Leung, Z. Islam, R.M. Kooistra, I. Parikh, E. Marion, G.J. Knott, J.A. Doudna, A.M. Le Ny, D. Madan, Kinetic analysis of Cas12a and Cas13a RNA-Guided nucleases for development of improved CRISPR-Based diagnostics, iScience 24 (2021), 102996. https://doi.org/10.1016/j.isci.2021.102996.
[129] H. Li, X. Cui, L. Sun, X. Deng, S. Liu, X. Zou, B. Li, C. Wang, Y. Wang, Y. Liu, B. Lu, B. Cao, High concentration of Cas12a effector tolerates more mismatches on ssDNA, Faseb. J. 35 (2021), e21153. https://doi.org/10.1096/fj.202001475R.
[130] B.X.H. Fu, J.D. Smith, R.T. Fuchs, M. Mabuchi, J. Curcuru, G.B. Robb, A.Z. Fire, Target-dependent nickase activities of the CRISPR-Cas nucleases Cpf1 and Cas9, Nat. Microbiol. 4 (2019) 888–897. https://doi.org/10.1038/s41564-019-0382-0.
[131] K. Murugan, A.S. Seetharam, A.J. Severin, D.G. Sashital, CRISPR-Cas12a has widespread off-target and dsDNA-nicking effects, J. Biol. Chem. 295 (2020) 5538–5553. https://doi.org/10.1074/jbc.RA120.012933.
[132] H. Kim, W.J. Lee, Y. Oh, S.H. Kang, J.K. Hur, H. Lee, W. Song, K.S. Lim, Y.H. Park, B.S. Song, Y.B. Jin, B.H. Jun, C. Jung, D.S. Lee, S.U. Kim, S.H. Lee, Enhancement of target specificity of CRISPR-Cas12a by using a chimeric DNA-RNA guide, Nucleic Acids Res. 48 (2020) 8601–8616. https://doi.org/10.1093/nar/gkaa605.
[133] B.P. Kleinstiver, A.A. Sousa, R.T. Walton, Y.E. Tak, J.Y. Hsu, K. Clement, M.M. Welch, J.E. Horng, J. Malagon-Lopez, I. Scarfò, M.V. Maus, L. Pinello, M.J. Aryee, J.K. Joung, Engineered CRISPR-Cas12a variants with increased activities and improved targeting ranges for gene, epigenetic and base editing, Nat. Biotechnol. 37 (2019) 276–282. https://doi.org/10.1038/s41587-018-0011-0.
[134] S.Y. Li, Q.X. Cheng, J.M. Wang, X.Y. Li, Z.L. Zhang, S. Gao, R.B. Cao, G.P. Zhao, J. Wang, CRISPR-Cas12a-assisted nucleic acid detection, Cell Discov. 4 (2018) 20. https://doi.org/10.1038/s41421-018-0028-z.
[135] M.C. Marqués, R. Ruiz, R. Montagud-Martínez, R. Márquez-Costa, S. Albert, P. Domingo-Calap, G. Rodrigo, CRISPR-Cas12a-based detection of SARS-CoV-2 harboring the E484K mutation, ACS Synth. Biol. 10 (2021) 3595–3599. https://doi.org/10.1021/acssynbio.1c00323.
[136] Y. Liang, L. Zou, H. Lin, B. Li, J. Zhao, H. Wang, J. Sun, J. Chen, Y. Mo, X. Yang, X. Deng, S. Tang, Detection of major SARS-CoV-2 variants of concern in clinical samples via CRISPR-Cas12a-mediated mutation-specific assay, ACS Synth. Biol. 11 (2022) 1811–1823. https://doi.org/10.1021/acssynbio.1c00643.
[137] P. Li, J. Zhang, Q. Lin, J. Kong, X. Fang, Rapid differential diagnosis of the B.1.617.2 (delta) variant of SARS-CoV-2 using an automated Cas12a-microfluidic system, Chem. Commun. 57 (2021) 12270–12272. https://doi.org/10.1039/d1cc04874k.
[138] H. de Puig, R.A. Lee, D. Najjar, X. Tan, L.R. Soeknsen, N.M. Angenent-Mari, N.M. Donghia, N.E. Weckman, A. Ory, C.F. Ng, P.Q. Nguyen, A.S. Mao, T.C. Ferrante, G. Lansberry, H. Sallum, J. Niemi, J.J. Collins, Minimally instrumented SHERLOCK (miSHERLOCK) for CRISPR-based point-of-care diagnosis of SARS-CoV-2 and emerging variants, Sci. Adv. 7 (2021), eabh2944. https://doi.org/10.1126/sciadv.abh2944.
[139] L.T. Nguyen, N.C. Macaluso, B.L.M. Pizzano, M.N. Cash, J. Spacek, J. Karasek, M.R. Miller, J.A. Lednicky, R.R. Dinglasan, M. Salemi, P.K. Jain, A thermostable Cas12b from Brevibacillus leverages one-pot discrimination of SARS-CoV-2 variants of concern, EBioMedicine 77 (2022), 103926. https://doi.org/10.1016/j.ebiom.2022.103926.
[140] Z. Chen, J. Li, T. Li, T. Fan, C. Meng, C. Li, J. Kang, L. Chai, Y. Hao, Y. Tang, O.A. Al-Hartomy, S. Wageh, A.G. Al-Sehemi, Z. Luo, J. Yu, Y. Shao, D. Li, S. Feng, W.J. Liu, Y. He, X. Ma, Z. Xie, H. Zhang, A CRISPR/Cas12a-empowered surface plasmon resonance platform for rapid and specific diagnosis of the Omicron variant of SARS-CoV-2, Natl. Sci. Rev. 9 (2022), nwac104. https://doi.org/10.1093/nsr/nwac104.
[141] C. Blanluet, D.A. Huyke, A. Ramachandran, A.S. Avaro, J.G. Santiago, Detection and discrimination of single nucleotide polymorphisms by quantification of CRISPR-Cas catalytic efficiency, Anal. Chem. 94 (2022) 15117–15123. https://doi.org/10.1021/acs.analchem.2c03338.
[142] C. He, C. Lin, G. Mo, B. Xi, A.A. Li, D. Huang, Y. Wan, F. Chen, Y. Liang, Q. Zuo, W. Xu, D. Feng, G. Zhang, L. Han, C. Ke, H. Du, L. Huang, Rapid and accurate detection of SARS-CoV-2 mutations using a Cas12a-based sensing platform, Biosens. Bioelectron. 198 (2022), 113857. https://doi.org/10.1016/j.bios.2021.113857.
[143] H. Lin, Y. Liang, L. Zou, B. Li, J. Zhao, H. Wang, J. Sun, X. Deng, S. Tang, Combination of isothermal recombinase-aided amplification and CRISPR-Cas12a-mediated assay for rapid detection of major severe acute respiratory syndrome coronavirus 2 variants of concern, Front. Microbiol. 13 (2022), 945133. https://doi.org/10.3389/fmicb.2022.945133.
[144] T. Zhang, W. Zhao, X. Chen, X. Zhang, J. Zhu, S. Li, C. Wu, Z. Tian, G. Sui, Fully automated CRISPR-LAMP platform for SARS-CoV-2 Delta and Omicron variants, Anal. Chem. 94 (2022) 15472–15480. https://doi.org/10.1021/acs.analchem.2c03607.
[145] Y. Liang, H. Lin, L. Zou, X. Deng, S. Tang, Rapid detection and tracking of Omicron variant of SARS-CoV-2 using CRISPR-Cas12a-based assay, Biosens. Bioelectron. 205 (2022), 114098. https://doi.org/10.1016/j.bios.2022.114098.
[146] C.L. Fasching, V. Servellita, B. McKay, V. Nagesh, J.P. Broughton, A. Sotomayor-Gonzalez, B. Wang, N. Brazer, K. Reyes, J. Streithorst, R.N. Deraney, E. Stanfield, C.G. Hendriks, B. Fung, S. Miller, J. Ching, J.S. Chen, C.Y. Chiu, COVID-19 variant detection with a high-fidelity CRISPR-Cas12 enzyme, J. Clin. Microbiol. 60 (2022), e00261–22. https://doi.org/10.1128/jcm.00261-22.
[147] A.A. Smargon, D.B.T. Cox, N.K. Pyzocha, K.J. Zheng, I.M. Slaymaker, J.S. Gootenberg, O.A. Abudayyeh, P. Essletzbichler, S. Shmakov, K.S. Makarova, E.V. Koonin, F. Zhang, Cas13b is a type VI-B CRISPR-associated RNA-guided RNase differentially regulated by accessory proteins Csx27 and Csx28, Mol. Cell 65 (2017) 618–630. https://doi.org/10.1016/j.molcel.2016.12.023.
[148] W.X. Yan, S. Chong, H. Zhang, K.S. Makarova, E.V. Koonin, D.R. Cheng, D.A. Scott, Cas13d is a compact RNA-targeting type VI CRISPR effector

positively modulated by a WYL-domain-containing accessory protein, Mol. Cell 70 (2018) 327–339. https://doi.org/10.1016/j.molcel.2018.02.028.
[149] S. Shmakov, A. Smargon, D. Scott, D. Cox, N. Pyzocha, W. Yan, O.O. Abudayyeh, J.S. Gootenberg, K.S. Makarova, Y.I. Wolf, K. Severinov, F. Zhang, E.V. Koonin, Diversity and evolution of class 2 CRISPR-Cas systems, Nat. Rev. Microbiol. 15 (2017) 169–182. https://doi.org/10.1038/nrmicro.2016.184.
[150] O.O. Abudayyeh, J.S. Gootenberg, P. Essletzbichler, S. Han, J. Joung, J.J. Belanto, V. Verdine, D.B.T. Cox, M.J. Kellner, A. Regev, E.S. Lander, D.F. Voytas, A.Y. Ting, F. Zhang, RNA targeting with CRISPR-Cas13, Nature 550 (2017) 280–284. https://doi.org/10.1038/nature24049.
[151] J.S. Gootenberg, O.O. Abudayyeh, M.J. Kellner, J. Joung, J.J. Collins, F. Zhang, Multiplexed and portable nucleic acid detection platform with Cas13, Cas12a, and Csm6, Science 360 (2018) 439–444. https://doi.org/10.1126/science.aaq0179.
[152] C. Myhrvold, C.A. Freije, J.S. Gootenberg, O.O. Abudayyeh, H.C. Metsky, A.F. Durbin, M.J. Kellner, A.L. Tan, L.M. Paul, L.A. Parham, K.F. Garcia, K.G. Barnes, B. Chak, A. Mondini, M.L. Nogueira, S. Isern, S.F. Michael, I. Lorenzana, N.L. Yozwiak, B.L. MacInnis, I. Bosch, L. Gehrke, F. Zhang, P.C. Sabeti, Field-deployable viral diagnostics using CRISPR-Cas13, Science 360 (2018) 444–448. https://doi.org/10.1126/science.aas8836.
[153] Y. Shan, X. Zhou, R. Huang, D. Xing, High-fidelity and rapid quantification of miRNA combining crRNA programmability and CRISPR/Cas13a trans-cleavage activity, Anal. Chem. 91 (2019) 5278–5285. https://doi.org/10.1021/acs.analchem.9b00073.
[154] M. Patchsung, K. Jantarug, A. Pattama, K. Aphicho, S. Suraritdechachai, P. Meesawat, K. Sappakhaw, N. Leelahakorn, T. Ruenkam, T. Wongsatit, N. Athipanyasilp, B. Eiamthong, B. Lakkanasirorat, T. Phoodokmai, N. Niljianskul, D. Pakotiprapha, S. Chanarat, A. Homchan, R. Tinikul, P. Kamutira, K. Phiwkaow, S. Soithongcharoen, C. Kantiwiriyawanitch, V. Pongsupasa, D. Trisrivirat, J. Jaroensuk, T. Wongnate, S. Maenpuen, P. Chaiyen, S. Kamnerdnakta, J. Swangsri, S. Chuthapisith, Y. Sirivatanauksorn, C. Chaimayo, R. Sutthent, W. Kantakamalakul, J. Joung, A. Ladha, X. Jin, J.S. Gootenberg, O.O. Abudayyeh, F. Zhang, N. Horthongkham, C. Uttamapinant, Clinical validation of a Cas13-based assay for the detection of SARS-CoV-2 RNA, Nat. Biomed. Eng. 4 (2020) 1140–1149. https://doi.org/10.1038/s41551-020-00603-x.
[155] L. Liu, X. Li, J. Wang, M. Wang, P. Chen, M. Yin, J. Li, G. Sheng, Y. Wang, Two distant catalytic sites are responsible for C2c2 RNase activities, Cell 168 (2017) 121–134. https://doi.org/10.1016/j.cell.2016.12.031.
[156] T. Zhou, R. Huang, M. Huang, J. Shen, Y. Shan, D. Xing, CRISPR/Cas13a powered portable electrochemiluminescence chip for ultrasensitive and specific MiRNA detection, Adv. Sci. 7 (2020), 1903661. https://doi.org/10.1002/advs.201903661.
[157] Y. Ke, S. Huang, B. Ghalandari, S. Li, A.R. Warden, J. Dang, L. Kang, Y. Zhang, Y. Wang, Y. Sun, J. Wang, D. Cui, X. Zhi, X. Ding, Hairpin-spacer crRNA-enhanced CRISPR/Cas13a system promotes the specificity of single nucleotide polymorphism (SNP) identification, Adv. Sci. 8 (2021), 2003611. https://doi.org/10.1002/advs.202003611.
[158] H.C. Metsky, N.L. Welch, P.P. Pillai, N.J. Haradhvala, L. Rumker, S. Mantena, Y.B. Zhang, D.K. Yang, C.M. Ackerman, J. Weller, P.C. Blainey, C. Myhrvold, M. Mitzenmacher, P.C. Sabeti, Designing sensitive viral diagnostics with machine learning, Nat. Biotechnol. 40 (2022) 1123–1131. https://doi.org/10.1038/s41587-022-01213-5.
[159] H. Shinoda, T. Iida, A. Makino, M. Yoshimura, J. Ishikawa, J. Ando, K. Murai, K. Sugiyama, Y. Muramoto, M. Nakano, K. Kiga, L. Cui, O. Nureki, H. Takeuchi, T. Noda, H. Nishimasu, R. Watanabe, Automated amplification-free digital RNA detection platform for rapid and sensitive SARS-CoV-2 diagnosis, Commun. Biol. 5 (2022) 473. https://doi.org/10.1038/s42003-022-03433-6.
[160] M. Niu, Y. Han, X. Dong, L. Yang, F. Li, Y. Zhang, Q. Hu, X. Xia, H. Li, Y. Sun, Highly sensitive detection method for HV69-70del in SARS-CoV-2 Alpha and Omicron variants based on CRISPR/Cas13a, Front. Bioeng. Biotechnol. 10 (2022), 831332. https://doi.org/10.3389/fbioe.2022.831332.
[161] N.L. Welch, M. Zhu, C. Hua, J. Weller, M.E. Mirhashemi, T.G. Nguyen, S. Mantena, M.R. Bauer, B.M. Shaw, C.M. Ackerman, S.G. Thakku, M.W. Tse, J. Kehe, M.M. Uwera, J.S. Eversley, D.A. Bielwaski, G. McGrath, J. Braidt, J. Johnson, F. Cerrato, G.K. Moreno, L.A. Krasilnikova, B.A. Petros, G.L. Gionet, E. King, R.C. Huard, S.K. Jalbert, M.L. Cleary, N.A. Fitzgerald, S.B. Gabriel, G.R. Gallagher, S.C. Smole, L.C. Madoff, C.M. Brown, M.W. Keller, M.M. Wilson, M.K. Kirby, J.R. Barnes, D.J. Park, K.J. Siddle, C.T. Happi, D.T. Hung, M. Springer, B.L. MacInnis, J.E. Lemieux, E. Rosenberg, J.A. Branda, P.C. Blainey, P.C. Sabeti, C. Myhrvold, Multiplexed CRISPR-based microfluidic platform for clinical testing of respiratory viruses and identification of SARS-CoV-2 variants, Nat. Med. 28 (2022) 1083–1094. https://doi.org/10.1038/s41591-022-01734-1.
[162] B. Casati, J.P. Verdi, A. Hempelmann, M. Kittel, A.G. Klaebisch, B. Meister, S. Welker, S. Asthana, S. Di Giorgio, P. Boskovic, K.H. Man, M. Schopp, P.A. Ginno, B. Radlwimmer, C.E. Stebbins, T. Miethke, F.N. Papavasiliou, R. Pecori, Rapid, adaptable and sensitive Cas13-based COVID-19 diagnostics using ADESSO, Nat. Commun. 13 (2022) 3308. https://doi.org/10.1038/s41467-022-30862-y.
[163] A. Tambe, A. East-Seletsky, G.J. Knott, J.A. Doudna, M.R. O'Connell, RNA binding and HEPN-nuclease activation are decoupled in CRISPR-Cas13a, Cell Rep. 24 (2018) 1025–1036. https://doi.org/10.1016/j.celrep.2018.06.105.
[164] R.T. Walton, K.A. Christie, M.N. Whittaker, B.P. Kleinstiver, Unconstrained genome targeting with near-PAMless engineered CRISPR-Cas9 variants, Science 368 (2020) 290–296. https://doi.org/10.1126/science.aba8853.
[165] D. Collias, C.L. Beisel, CRISPR technologies and the search for the PAM-free nuclease, Nat. Commun. 12 (2021) 555. https://doi.org/10.1038/s41467-020-20633-y.